NASA CONTRACTOR REPORT

NASA CR-988

NASA CR-988

N68-13115
(ACCESSION NUMBER) (THRU)
60 1
(PAGES) (CODE)
23
(NASA CR OR TMX OR AD NUMBER) (CATEGORY)
FF No. 602(B)

DESIGN AND CONSTRUCTION OF AN ENGINEERING MODEL SOLID CRYOGEN REFRIGERATOR FOR INFRARED DETECTOR COOLING AT 50° K

by R. P. Caren and R. M. Coston

Prepared by
LOCKHEED MISSILES AND SPACE COMPANY
Palo Alto, Calif.
for Goddard Space Flight Center

NATIONAL AERONAUTICS AND SPACE ADMINISTRATION • WASHINGTON, D. C. • JANUARY 1968

NASA CR-988

DESIGN AND CONSTRUCTION OF AN ENGINEERING MODEL SOLID CRYOGEN REFRIGERATOR FOR INFRARED DETECTOR COOLING AT 50° K

By R. P. Caren and R. M. Coston

Distribution of this report is provided in the interest of information exchange. Responsibility for the contents resides in the author or organization that prepared it.

Prepared under Contract No. NAS 5-9549 by
LOCKHEED MISSILES AND SPACE COMPANY
Palo Alto, Calif.

for Goddard Space Flight Center

NATIONAL AERONAUTICS AND SPACE ADMINISTRATION

For sale by the Clearinghouse for Federal Scientific and Technical Information
Springfield, Virginia 22151 – CFSTI price $3.00

PRECEDING PAGE BLANK NOT FILMED.

FOREWORD

This report was prepared by the Thermophysics Section of the Aerospace Sciences Laboratory, Lockheed Missiles and Space Company, Research Laboratory for the Aeronomy and Meteorology Branch of NASA Goddard Space Flight Center. The work was performed under Contract NAS 5-9549, in the time period from 15 June 1965 to March 24, 1967.

The program was carried out under the direction of R. P. Caren with R. M. Coston as the Chief Project Scientist. The construction of the refrigerator was principally the work of R. E. Barrow with assistance from C. A. Jernberg and L. Lambert.

PRECEDING PAGE BLANK NOT FILMED.

CONTENTS

Section		Page
	FOREWORD	iii
	ILLUSTRATIONS	vi
	NOMENCLATURE	ix
1.0	General Technical Background	1
2.0	Technical Objectives	2
3.0	Technical Methods	3
	3.1 Structural and Thermal Design of Solid Cryogen Refrigerator	4
	3.1.1 Structural Design of Solid Cryogen Refrigerator	4
	3.1.2 Thermal Design of Solid Cryogen Refrigerator	11
	3.2 Argon Solidification and Cooling Technique	12
	3.3 Passive Detector Temperature Regulation	14
	3.4 Solid Carbon Dioxide Solidification Technique	19
	3.5 Detector Mounting and Electrical Leads	22
	3.6 Refrigerator Servicing Module	24
4.0	Solid Cryogen Refrigerator Fabrication	29
5.0	Solid Cryogen Refrigerator Characteristics Tests	40
	5.1 Solid Cryogen Refrigerator Thermal Characteristics Tests	40
	5.2 Solid Cryogen Refrigerator Mechanical Characteristics Tests	47
6.0	Summary, Conclusions and Recommendations	48
7.0	References	55

ILLUSTRATIONS

Table		Page
1	Solid Cryogen Refrigerator Design Characteristics	6
2	Argon Venting Tube Diameters vs. Tube Length	17
3	Predicted vs. Measured Characteristics of Solid Cryogen Refrigerator	50
4	Comparison of Properties of Argon and Methane	53

Figure		
1	Schematic of Solid Argon-Solid Carbon Dioxide Infrared Detector Refrigerator	5
2	Energy Balance for Argon System vs. Carbon Dioxide Equilibrium Temperature	13
3	Argon Vapor Pressure vs Temperature	16
4	Carbon Dioxide Pressure vs. Temperature	21
5	Carbon Dioxide Venting Tube Dimensions vs. Carbon Dioxide Temperature	23
6	Resistance vs. Temperature for Platinum Resistance Thermometer on Detector Rod	25
7	Solid Cryogen Refrigerator Servicing System Schematics	27
8	Bottom View of Argon Container	31
9	Internal View of Argon Container	31
10	Top View of Argon Container	31
11	Side View of Argon Container	31
12	Side View of Carbon Dioxide Container	33
13	Top View of Carbon Dioxide Container	33
14	Bottom View of Carbon Dioxide Container	33
15	Argon Vent Tube System	33
16	Support Cage for Multilayer Insulation	36
17	Support Cage for Floating Radiation Shield	36
18	Top View of Uninsulated Refrigerator Assembly	37

ILLUSTRATIONS CONT'D.

Figure		Page
19	Side View of Uninsulated Refrigerator Assembly	37
20	Side View of Insulated Refrigerator Assembly	37
21	Refrigerator Service Model	37
22	Multilayer Insulation Conductivity as a Function of Density	43
23	Detector Temperature vs Time During Cooldown	43
24	Refrigerator Acceleration vs Frequency for a 1 g Acceleration Input	49

PRECEDING PAGE BLANK NOT FILMED.

NOMENCLATURE

Q	heat flux
P	vapor pressure over cryogen
T	temperature of cryogen
D	cryogen vapor venting tube diameter
L	cryogen vapor venting tube length
$\mathcal{L}$	cryogen latent head of sublimation
$\dot{m}$	cryogen vapor mass venting rate
$\bar{T}$	average temperature of cryogen vapor in venting tube
$\bar{\eta}$	average viscosity of cryogen vapor in venting tube
$\bar{P}$	average pressure of cryogen vapor in venting tube
$\bar{\rho}$	average density of cryogen vapor in venting tube
C_s	specific heat at saturation pressure of cryogen vapor
M	molecular weight of cryogen
P_o	pressure at downstream side of vent tube

1.0 General Technical Background

In order to efficiently detect infrared radiation in the wavelength range out to 10 microns, cooled photoconducting detectors are required. To detect this long wavelength infrared radiation impurity rather than intrinsic semiconductors must be utilized. In an intrinsic semiconductor photoconductivity is generally caused by the excitation of electrons from the valence band to the conduction band by quanta of incident radiation. The long wavelength limit of photoconduction is then determined by the fact that the incident quanta must have an energy at least as large as the band gap energy between the valence and conduction bands. However, the usual intrinsic photoconducting detectors such as PbS, PbSe, and PbTe have band gaps corresponding to maximum detectable wavelengths in the 5 to 7 micron range.

Doped or impurity semiconductors, on the other hand, have energy levels associated with the impurity atoms occupying positions in the energy band scheme between the valence and conduction bands of the parent material. Because of their position in the forbidden energy zone, transitions in which these levels either donate electrons to the conduction band or accept electrons from the valence band involve smaller excitation energies than the intrinsic transitions from valence to conduction band. Thus, certain doped semiconductors have much longer wavelength detection limits than intrinsic photoconductors. However, extrinsic type photoconductors require cooling to preclude thermal excitation of the impurity levels and hence thermal saturation of the detector. For extrinsic photoconductors having long wavelength limits in the 10 micron range, the detector should be operated at or below approximately $50^{\circ}K$ in order to preclude thermal saturation. Examples of extrinsic photoconductive detectors operable from the visible wavelength range out to 10 microns, which are operable at $50^{\circ}K$ include antimony and zinc doped germanium and germanium-silicon alloys doped with either gold or antimony and zinc.

For infrared detectors requiring refrigeration at or below $50^{\circ}K$ the problem of supplying the refrigeration on board spacecraft is formidable, particularly in view of stringent requirements, such as low system weight, power, volume,

and high system lifetime and reliability. Conventional means of refrigeration are easily shown to be inapplicable on the basis of power requirements, low reliability, and excessive weight for all but short term missions. The only systems presently capable of providing the refrigeration of infrared detectors aboard spacecraft for long term missions are either liquid or solid cryogens. In either case, in order that the principal heat load to the cryogen will be the detector, a multilayer insulation plus low thermal conductivity support systems must be provided for proper thermal isolation of the cryogen. For spacecraft infrared detector cooling requirements a solid cryogen is more favorable than the same cryogen in the liquid state for the following reasons:

- In the zero "g" conditions of spacecraft there is no venting problem in the case of a solid, only the vapor from the subliming solid would be vented; whereas for the liquid phase their could be liquid venting and a resulting loss in refrigeration capacity.
- In the solid system the latent heat of vaporization is available for refrigeration systems. For most cryogens this is a 10 to 15 per cent gain in refrigeration capacity. Also, there is a 10 to 15 per cent gain in the density of the cryogen in the solid phase. Thus, for a solid, there is a 20 to 30 per cent gain in refrigeration capacity per unit volume over that available with the same cryogen in a liquid state.
- The lower temperature of the solid phase permits a gain in infrared detector system sensitivity.

2.0 Technical Objectives

The objective of this program was the construction of a prototype spacecraft solid cryogen refrigerator capable of providing of cooling at a temperature of approximately 50°K for an infrared detector. The refrigerator was to provide this requisite cooling for a period of 1 year based on a refrigerator outer skin temperature of 300°K. The total system weight, excluding the outer vacuum jacket, was to be approximately 30 lbs. In a flight unit, during ground hold, the insulation system would not be evacuated but surrounded by a helium or neon purged mylar bag to prevent air condensation. During the spacecraft boost phase the purge bag would be automatically evacuated

The refrigerator was to occupy a small volume. The detector temperature was to be regulated either actively or passively both for changes of the detector heat load and also over the refrigerator lifetime. The structure of the refrigerator was to be designed to withstand launch acceleration and vibration as specified in the document, "An Environmental Specification for a Meteorologically Spacecraft Subsystem," prepared by NASA/GSFC.

3.0 Technical Methods

The $50^{\circ}K$ refrigerating power is supplied to the infrared detector via a copper thermal link from a container of solid argon held at approximately $50^{\circ}K$. The $50^{\circ}K$ solid argon temperature is maintained by the choice of the proper conductance of the gaseous argon venting path to the space vacuum environment. The use of a gaseous venting path conductance for fixing the operating temperature of the detector also provides passive temperature regulation.

Since the solid argon required for 1 year's detector cooling is the dominate system weight, the argon requirement is minimized by reducing as much as possible all extraneous heat leaks to the solid argon. Solid carbon dioxide in conjunction with a surrounding evacuated multilayer insulation is used to provide a low temperature radiative boundary surrounding the solid argon. This low temperature radiative boundary surrounding the argon significantly reduces the extraneous heat flow to the argon. If a carbon dioxide thermal protection system were not used the argon required would be increased by a factor of three. A refrigerator using argon alone would weigh 15 to 20 lbs. more than the present argon-carbon dioxide system. The utility of a carbon dioxide thermal protection system lies in the fact that the latent heat of sublimation of carbon dioxide is approximately three times that of argon on either a volumetric or mass basis. The equivalence of the latent heats on both a volumetric and mass basis is due to the equal densities of argon and carbon dioxide (1.7 g/cc). The support system for the argon container is non-metallic in order to utilize the lower thermal conductivity to strength ratios of non-metallic materials. The argon structural support system is thermally grounded to the solid carbon dioxide container to utilize the reduction in the thermal conductivity integral between solid carbon dioxide ($125^{\circ}K$) and solid argon temperatures over that between

room temperature (296°K) and solid argon temperature.

3.1 Structural and Thermal Design of Solid Cryogen Refrigerator

The structural and thermal design of a spaceborne sublimating solid refrigerator are not two independent tasks. In fact, the rigidity required of structures to withstand the ascent environment are in distinct contrast to the thin walled low conductivity supporting members used in cryogen storage containers. Hence, in any minimum weight, flight qualified, cryogen storage system there must be a strong counterplay between the thermal and structural requirements of the system. Thus, for example for the supporting members for the cryogen containers in the present system glass reinforced epoxy tubes are utilized, due to their superior strength to thermal conductivity ratio as compared to metals.

Several different cryogen container-structural configurations were considered as part of the refrigerator system design. The conclusion was reached that a design using concentric containers, in the order of argon container, vacuum space, carbon dioxide container, insulation space, is more complex, has more container weight, and is more difficult to fabricate than a system utilizing two stacked cylindrical cryogen containers and a common vacuum space for the containers and the insulation system. Thus, the latter design was chosen for the present prototype solid cryogen refrigerator system. This stacked design is shown schematically in Figure 1 and its thermal and structural aspects are described in the two following subsections. This design is particularly attractive also because the structural support for the refrigerator and the support systems between the cryogen containers are long which reduces heat transfer via these paths.

3.1.1 Structural Design of Solid Cryogen Refrigerator

The design characteristics of the presently considered subliming refrigerator design are summarized in Table 1. This design is based on a sensor operating temperature of 50°K for a duration of one year and an approximate system weight of 30 lbs. From these basic parameters and for this design a detector heat load of 25 milliwatts is permissible for a carbon dioxide cryogen temperature of 125°K.

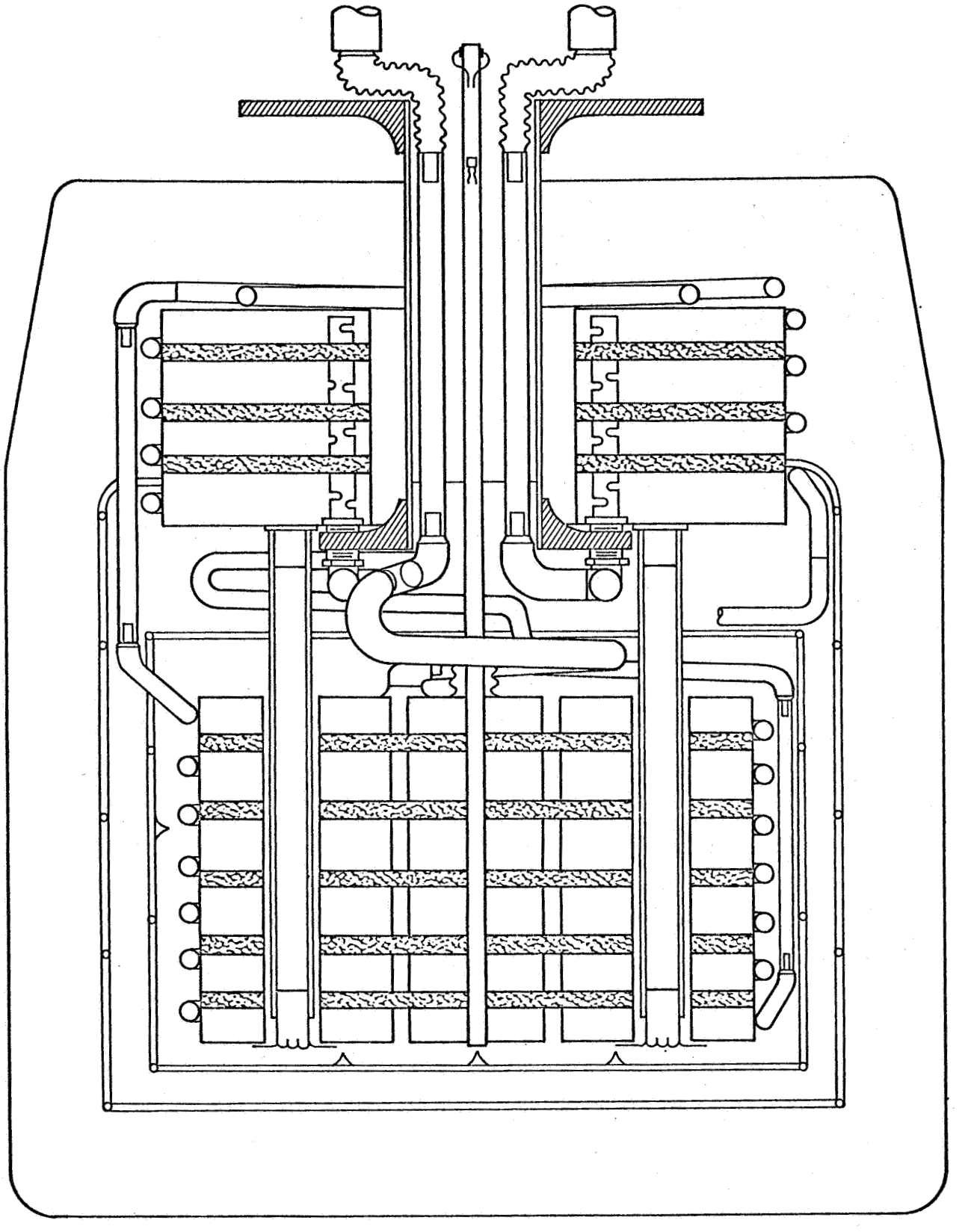

Figure 1. Schematic of Solid Argon-Solid Carbon Dioxide Infrared Detector Refrigerator

Table 1

Subliming Refrigerator Design Characteristics

	Infrared Detector Cooling Capacity
Temperature, ^{o}K	50
Duration, years	1
Heat Load, Milliwatts	25

Refrigerator System Characteristics

	Refrigerants	
	Primary Argon	Secondary CO_2
	Containers Specifications	
Volume, in^3	223	150
Dimensions	8.2"O.D. x 5" High	9.2"O.D. x 3.0 I.D. x 4.25" High
	Container and Refrigerant Weights	
Container	1.7	1.2
Refrigerants	13.7	8.8
	Heat Transfer to Refrigerants	
Radiation	10	52
Supports	5	24
Detector	25	
Total	40	76

	Weight Summary of Systems, lbs
Refrigerants	22.5
Containers	2.9
Container Support	0.7
Detector Support and Window	.2
insulation	2.4
Heat Exchanger, Internal & External	.8
Radiation Shroud	.4
Total	29.9

In the structural design of the refrigerator which is shown schematically in Figure 1, the argon and carbon dioxide containers are constructed from thin stainless steel sheets. The sides and the ends of the container have wall thicknesses of 0.024 and 0.036 inches respectively. Initially, it was believed that the carbon dioxide container would have to withstand an internal pressure of at least 75 psi. This was because the most obvious means of producing high density solid carbon dioxide was to first liquefy the carbon dioxide near its triple point (the triple point of carbon dioxide occurs at a pressure of 75 psi and a temperature of 216°K) and then subcool the liquid to a solid using liquid nitrogen as the refrigerant. But experiments performed under this contract (See Section 3.4) showed that a high density carbon dioxide solid could be grown on a liquid nitrogen cooled wall directly from the gas phase at a pressure of 1 atmosphere. Thus, both argon and carbon dioxide containers were designed to support both external and internal pressures of at least 15 psia. The maximum internal pressure occurs during the servicing operation when the solid cryogens are being formed at a pressure up to 15 psia. The maximum external pressures occur during the leak detection check of the weldment of the cryogen containers and during the refrigerator warm-up phase, when an exchange gas is placed in the insulation space to degrade the thermal performance of the multilayer insulation.

As shown in Figure 1, the carbon dioxide container is located above the argon container and does not surround the outer boundary of the argon container. The carbon dioxide temperature radiative boundary surrounding the argon container is provided by a 1.5 mil copper shroud which entirely surrounds the argon container. A two-inch mantle of evacuated multilayer insulations thermally isolates the copper shroud and the carbon dioxide container from their warm surrounds. The apparent thermal conductivity of the insulation systems was assumed for the design to be 5.2×10^{-7} $\omega/cm^{o}K$ (3.0×10^{-5} BTU/Hr Ft ^{o}R). In order to support the copper shroud and multilayer insulation in the area of the argon container, a cage of 1/16" O.D. x .010" wall stainless steel tubing is provided which is structurally attached to the carbon dioxide container. This cage will adequately support the insulation and copper shroud during

ascent, and will maintain an annular spacing of 1/2 inch between the copper shroud and the argon container. A floating radiation shield is located between the radiation shroud and the argon container and has a construction similar to that of the radiation shroud.

As is depicted in Figure 1 the support for the carbon dioxide container is a cantilever beam with a fixed end support and concentrated load at full span. The material chosen for the neck support tube is an S-Glass filament wound structure impregnated with an epoxy resin. This choice was made after a combined structural thermal analysis indicated its advantages. The reported high strength of the filament wound fiberglas ($\approx$ 100,000 psi) as opposed to the reported strengths of fiberglas reinforced epoxies (15,000 psi) allows a much thinner structural support.[1,2,3,4] As the thermal conductivities of both materials are approximately the same, the effective reduction in cross-sectional areas of the support members allowed with the use of the filament wound structure greatly improves the heat transfer characteristics of the system. The beam has a constant internal diameter of 1.72 inches. In order to provide sufficient strength and minimum heat conduction, the beam is tapered from a thickness of .045 inches at its fixed end to .012 inches at its free end. Metal flanges are fastened to each end of the beam with epoxy adhesives and the beam can then be bolted to the refrigerator support flange and the carbon dioxide container.

This support column has been subjected to tension, compression and bending structural tests. In tension the support column was loaded to 900 lbs., which is equivalent to approximately a 30 g loading, with no signs of yielding. However, in compression the column buckled at a compressive load of 540 lbs, which is approximately equivalent to a 15 g load on the refrigerator. Buckling occurred where the wall thickness was 0.012 inches. In the bending tests the specimen failed at a point 1.5 inches above the lower support flange. Again, the failure being due to buckling at an equivalent loading of 15 g. All tests were conducted with the support column at room temperature. The heat leak from the 300°K boundary temperature to the carbon dioxide container via the beam support is 24 milliwatts. This design is based on minimizing the heat leak to the carbon dioxide and on a practical consideration of the minimum machinable thickness of a non-metallic material such as glass fiber epoxy laminate.

The header at the top of the refrigerator is provided with an "O" ring groove for sealing the Irtran window, and with orifices for the carbon dioxide and argon fill and vent tube and the liquid nitrogen heat exchanger tubes. All cryogen transfer tubes passing through the top header are reentrant to prevent their cooling the header and Irtran window. The annular area between the detector support rod and the filament wound support beam is used to route the four fill and vent lines. Two of the lines are for the LN_2 heat exchanger used for the solid carbon dioxide and argon production and one each for the carbon dioxide and argon container. The LN_2 heat exchanger inlet and outlet tubes are 1/4 inch internal diameter while both the argon and carbon dioxide fill and vent lines are 3/8 inch internal diameter. In order to eliminate heat leaks to the cryogen systems via the vent and fill lines the straight sections of tubing in the neck section are made of mylar. Mylar is used because it possesses a thermal conductivity an order of magnitude lower than stainless steel tubing.If stainless steel tubing were used for the fill and vent tubes a total heat leak to the cryogens of several milliwatts would result. This would constitute a significant heat leak to the refrigerants. On the other hand, when mylar tubing is used the total heat leak via these tubes is less than 1/2 milliwatts, which is not a significant thermal load. Sections of mylar tubing are also used, as shown in Figure 1, in the sections of the liquid nitrogen heat exchanger tubes between the argon and carbon dioxide containers. The use of continuous stainess steel tubing in this circuit would result in too much thermal contact between the cryogens. The use of sections of mylar tubing in this circuit provides good thermal isolation between the cryogens. This mylar tubing has been obtained from the Stone Paper Tube Co., Washington, D.C. and experimentally evaluated for leaks at both room temperature and at liquid nitrogen temperature. As a qualification test several samples of the mylar tubing with the ends epoxied to stainless steel tubing with Hysol 1-C white epoxy were temperature cycled up to 100 times between room and liquid nitrogen temperature. Both the tubing and the epoxy seal areas maintained vacuum integrity.

The argon container is supported from the bottom of the carbon dioxide container by three glass fiber epoxy laminate columns. These columns extend from headers at the bottom of the carbon dioxide container to headers at the bottom of the argon container. Thus, a long thermal path length through these supporting

members is provided. Recesses are provided in the argon container for clearance between these supporting columns of the argon container. The carbon dioxide and argon containers are maintained in axial alignment under lateral loads by a restraining system which is shown in Figures 10 and 11, this restraining system makes contact near the top of the argon support columns under lateral loads. This system causes lateral forces on the argon container to appear as a couple along its axis between the top of the argon container and its center of mass. The resulting forces in the columns between the top and bottom of the argon container appear principally as compression or tension loads. Only in the small section of these columns between the bottom of the carbon dioxide container and the top of the argon container do shear forces occur under lateral loads. This system minimizes the lateral motion of the argon container relative to the carbon dioxide container and thus stiffens entire system below the main support column. During static or zero gravity conditions there will be no contact between this system and the argon support columns and therefore no heat leak from the carbon dioxide to the argon container through this structure. Using three 1/2 inch diameter by 0.020 inch wall glass fiber epoxy laminate supporting columns the maximum tension or compression forces under 30 g axial and 10 g lateral loads can be withstood with a safety factor of 10. The heat conduction along these tubes is calculated to be 5 milliwatts. The glass epoxy laminates were chosen as the column material because of their relatively high strength to weight ratio and their low thermal conductivity. For these materials engineering information is available for design calculations. Further, the glass epoxy materials are easily machined and bonded to other materials with epoxy resins.

The total design weight for the refrigerator as shown in Table 1 is estimated as 29.9 lbs. This structure should be suitable for orbital flight and is designed to sustain loads of 30 g's acceleration along, and 10 g's acceleration normal to, the axis of the refrigerator with the following exception. As indicated, in the static tensile tests performed on one sample of the main support column although this member will sustain loads equivalent to 30 g's acceleration of the refrigerator in tension, i.e., along the refrigerator axis, and 15 g's normal to its axis, it will support only 15 g's in compression. Thus, in order to support the force equivalent to 30 g's acceleration of the refrigerator mass along the refrigerator axis in compression, it would appear that the

wall thickness of the present support column must be increased. It should be pointed out that the failure point on the column under the compressional load tests was at the low temperature end. At the carbon dioxide temperature of 125°K the strength of this section of the column could be increased 30 to 50 per cent.[1,3] On the basis of the reported tensile strength of filament wound epoxy impregnated materials, however, the failure in the present column must be due to structural imperfections. Thus, a quality assurance program in which the columns are selected on the basis of tensile tests performed to the 15 to 30 g's equivalent static forces should be sufficient to guarantee selection of columns in compliance with all structural specifications.

3.1.2 Thermal Design of Solid Cryogen Refrigerator

The predicted heat loads to both the solid argon and solid carbon dioxide containers are summarized in Table 1. The calculated heat loads on the solid argon and solid carbon dioxide containers were calculated to be 40 and 76 milliwatts, respectively. The heat transfer rate to the carbon dioxide container is 52 milliwatts via radiation and conduction through a 2-inch thickness of superinsulation and 24 milliwatts via the filament wound glass reinforced epoxy support column. The radiant heat load on the solid carbon dioxide is that through a two inch thickness of multilayer insulation with the previously indicated assumed thermal conductivity of 5.2×10^{-7} w/cm°K (3.0×10^{-5} BTU/Hr Ft °R). The operating temperature of the carbon dioxide for the present design was assumed to be 125°K.

As shown in Figure 1, the carbon dioxide container is located above the argon container and does not surround the outer boundary of the argon container. The carbon dioxide temperature radiative boundary of 125°K surrounding the argon container is provided by a 1.5 mil copper shroud supported by a cage made from 1/16 inch diameter x .005 wall stainless steel tubing. A floating radiation shield of similar construction to that of the carbon dioxide shroud is held in place between the shroud and the argon container by nylon thread supports. Vibration suppressors made of teflon are attached to the shroud and floating radiation shield and contact the argon container during maximum g loading conditions.

The computed heat transfer rate to the argon is 11 milliwatts via radiation heat transfer between the 125°K carbon dioxide cooled copper shroud and the 50°K temperature of the argon container. This assumes an emittance of .02 on the copper shroud, the floating radiation shield and argon containers external surface. Recent measurements made on the low temperature emittance of metals at LMSC[5] indicate that the emittance of copper and gold at these temperatures is approximately 0.01. Thus, the use of an assumed emittance of 0.02 is a highly conservative estimate. The stainless steel argon container is gold plated in order to achieve better radiative thermal isolation. For a system without the floating radiation shield the maximum amount of refrigeration available for the detector would be 14 milliwatts.

The detector heat load is determined from an energy balance on the argon container and is dependent on the carbon dioxide temperature and the degree of thermal isolation of the "floating" radiation shield. This energy balance is shown in Figure 2. For a free floating radiation shield the maximum detector heat load with the outer carbon dioxide temperature shield at 125°K would be 25 milliwatts. As indicated previously for a system without the floating radiation shield the maximum heat load for the detector would be 14 milliwatts with a 125°K carbon dioxide temperature. The detector heat load includes the detector bias current electrical heating plus the radiant heat load on the detector plus the detector mounting assembly.

3.2 Argon Solidification and Cooling Technique

The triple point temperature and pressure for argon are 83.77°K and 514.1 torr respectively.[6] Thus, at the temperature of liquid nitrogen boiling at atmospheric pressure, which is 77°K, argon is a solid. Laboratory experiments carried out under the present contract using a transparent (glass) container immersed in liquid nitrogen showed that if argon gas at room temperature is introduced into the container at a rate sufficient to keep the gas pressure in the container above 514 torr, then liquid argon is first produced. Not until the container is nearly filled with liquid argon is growth of solid argon from the nitrogen cooled walls outward into the bulk of the liquid observed. If the argon gas pressure over the argon in the container is maintained the container can be entirely filled with solid argon. The mass of

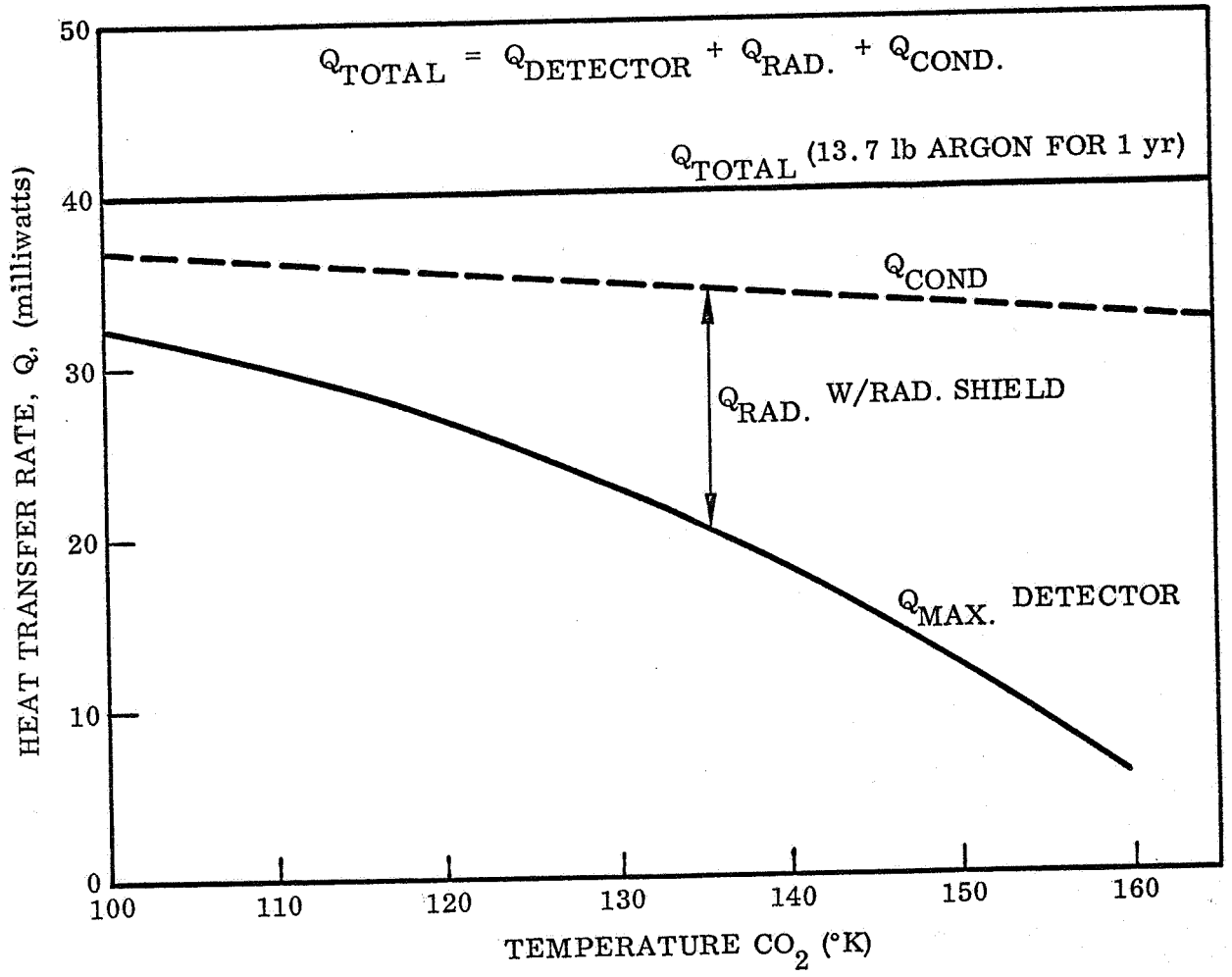

Figure 2. EnergyBalance for Argon System vs. Carbon Dioxide Equilibrium Temperature

argon transferred into the container in these experiments was determined by measuring the total argon gas flow into the container using a Precision wet test gas flowmeter. From a knowledge of the container volume the density of the solid argon achieved was determined to be 1.682 g/cc as compared to the density of 1.711 g/cc reported by Dobbs et al.[7] In view of this, the following method is used for producing a high density solid within the refrigerator. While an argon gas pressure in excess of 514 torr is maintained within the argon container, the container walls are cooled with liquid nitrogen flowing through a heat exchanger fashioned from 1/4 inch diameter stainless steel tubing soldered to the exterior container walls. This system liquefies the argon gas and subsequently cools the liquid to a solid mass. By maintaining the argon gas pressure voids which occur due to contraction of the solid are continuously filled. The use of Precision wet test gas flowmeters to meter total argon gas flow into the argon volume allow an accurate determination of the total mass of solid argon produced in the refrigerator.

In order to assure good thermal contact between the liquid nitrogen heat exchanger soldered to the refrigerator argon reservoir and the argon itself, the argon reservoir volume is partially filled with copper expanded foam. This metal foam serves several purposes:

- It produces good thermal contact between the liquid nitrogen heat exchanger and the argon during the initial liquefication and solidification processes.
- It allows uniform subcooling of the solid argon during the evaporative cooling from 77°K to the solid operating temperature.
- The copper thermal link between the infrared detector and the solid argon is soldered to the metal foam so that intimate thermal contact is provided between the detector and the solid argon.

3.3 Passive Detector Temperature Regulation

The copper thermal link between the infrared detector plus the expanded copper foam embedded in the solid argon provides intimate thermal contact between the detector and the solid argon. In the present system with the high degree

of thermal contact existing between the detector and the solid argon, which is maintained through the copper thermal link and expanded copper foam heat exchanger, the problem of maintaining the detector temperature is simply that of maintaining a relatively fixed temperature of the solid argon. This control of the solid argon temperature can, of course, be achieved by actively controlling the vapor pressure over the argon to its pressure corresponding to approximately $50^{\circ}K$. However, the saturation vapor pressure of argon at $50^{\circ}K$ is only 0.15 torr (See Fig. 3), so that any mechanical means for pressure control involving pressure actuated mechanisms will be cumbersome, heavy, and have questionalbe reliability. Therefore, the present system utilizes a totally passive temperature regulation scheme. This passive temperature regulation system essentially consists of the solid argon plus a vent line of fixed conductance leading to the space vacuum environment. This line is sized so that, with the normal heat flux Q to the solid, a pressure drop corresponding to a solid argon temperature of $50^{\circ}K$ provides the proper gaseous argon mass flow rate $\overset{\circ}{m}$. Thus,

$$\overset{\circ}{m} = \frac{Q}{\mathcal{L}}$$

If the heat input to the solid argon changes, i.e., if the detector heat load changes, then $\overset{\circ}{m}$ must change. The system passively produces the new equilibrium by changing the vapor pressure over the cryogen to accommodate the new mass flow rate. The passive system accomplishes this change in pressure by assuming a new solid argon equilibrium temperature. As will be shown for the $50^{\circ}K$ solid argon system, a very large change in heat load can be withstood without altering the initial equilibrium temperature more than $0.5^{\circ}K$. As previously stated, the mass flow rate from the solid argon will be directly proportional to the heat input Q for equilibrium; that is $Q = \mathcal{L}\overset{\circ}{m}$. For the venting system under consideration the vapor flow is laminar and $\overset{\circ}{m}$ is given to a very good degree of approximation by Poisuille's equation

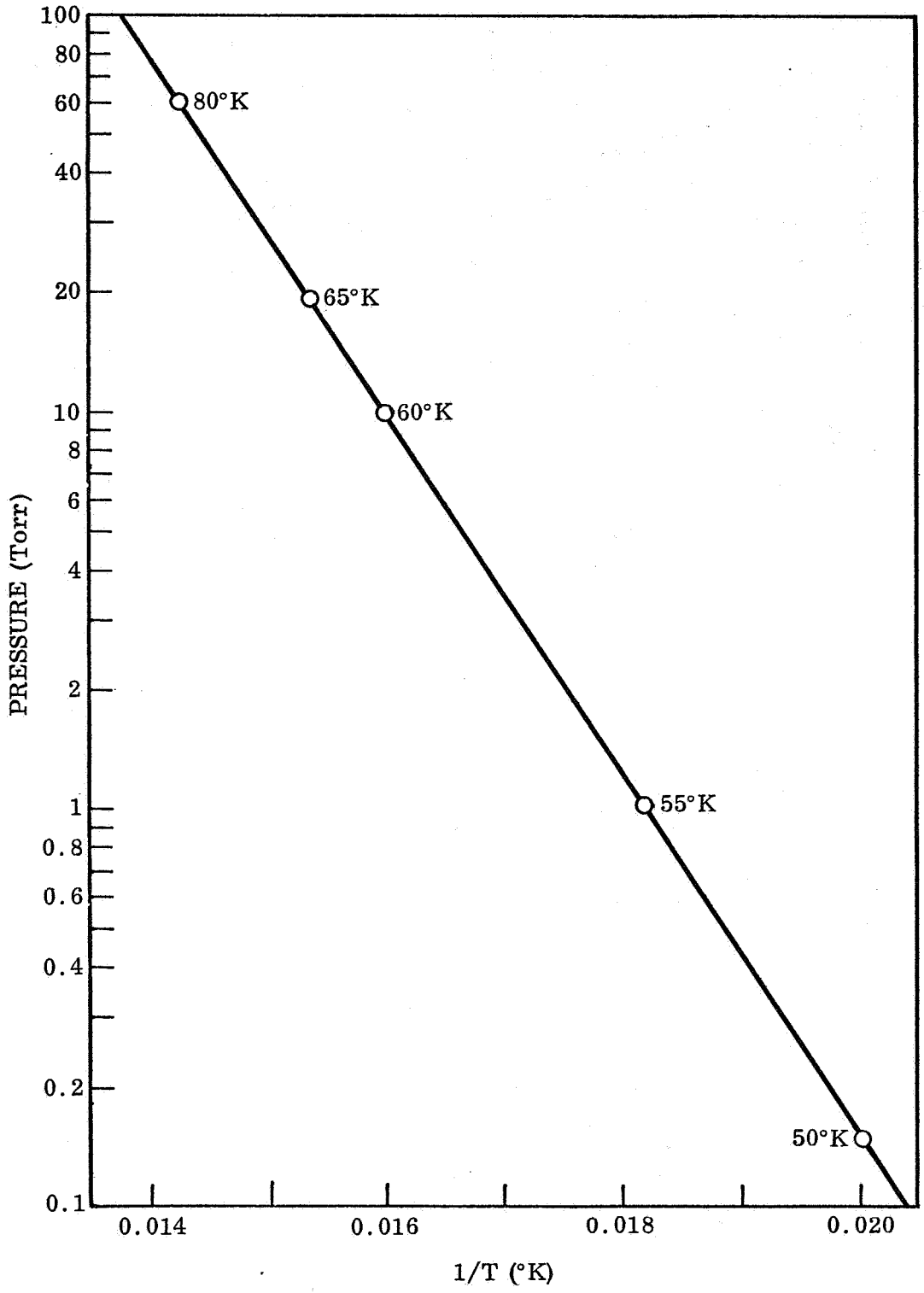

Figure 3. Argon Vapor Pressure vs. Temperature

$$\overset{o}{m} = \frac{\bar{\rho}\, D^4}{128\, \bar{\eta}\, L} (P - P_o)$$

Now, since the venting is into a vacuum, $P_o = 0$ and

$$Q = \mathcal{L}\, \overset{o}{m} = \mathcal{L}\, \frac{\pi D^4}{128\, \bar{\eta}\, L} P$$

Also, the average vapor density in the venting line $\bar{\rho}$ is given by

$$\bar{\rho} = \frac{\bar{P}M}{R\bar{T}} = \frac{1}{2} \frac{PM}{R\bar{T}}$$

$$Q = \mathcal{L}\, \overset{o}{m} = \mathcal{L}\, \frac{MD^4}{256\, R\bar{T}\, \bar{\eta}\, L} P^2$$

For a system venting 13.7 pounds of argon over the period of one year (see Section 3.1.2 for solid argon weight analysis) with an equilibrium argon temperature of 50^oK, this equation yields a value of the ratio of D^4/L of 1.2×10^{-3} in^3. Table 2 lists venting line diameters corresponding to various venting line lengths for this D^4/L ratio.

Table 2

Argon Venting Tube Diameters vs. Tube Length

L(in)	2	4	6	8
D(in)	.22	.26	.29	.31

A change in heat flux ΔQ is related to the corresponding change in vapor pressure over the solid ΔP by

$$\Delta Q \cong \frac{\pi M D^4}{256\ R\bar{T}\bar{\eta}\ L} \qquad 2P\Delta P$$

and the change in pressure is produced by a change in the solid argon temperature given by $\Delta P = \frac{dP}{dT}\ \Delta T$; thus

$$\frac{\Delta Q}{Q} = \frac{2\Delta P}{P} = \frac{2}{P}\ \frac{dP}{dT}\ \Delta T$$

Here it is evident that the expression which controls the percentage change of heat load which can be accommodated within a fixed detector temperature operating range ΔT is $\frac{1}{P}\ \frac{dP}{dT}$ which is greatest for a low temperature solid. Now, using the vapor pressure data for solid argon

$$\frac{1}{P}\ \frac{dP}{dT} = \frac{968}{T^2}$$

Hence,

$$\frac{\Delta Q}{Q} = \frac{1936}{T^2}\ \Delta T.$$

or

$$\frac{\Delta Q}{\Delta T} = \frac{1936}{T^2}\ Q$$

As has been previously indicated total allowed heat load on the argon for 1 year's operation of 40 milliwatts. Based on this heat load and a detector temperature operating temperature of approximately $50^{\circ}K$ it follows that

$\frac{\Delta Q}{\Delta T} \simeq 31$ mω/°K. Thus, for the assumed detector heat load of 25 mω a temperature variation of ±0.5°K in the nominal detector heat load corresponds to an allowable ± 15 mω variation in the nominal detector heat load of 25 mω.

3.4 Solid Carbon Dioxide Solidification Techniques

As previously indicated if solid carbon dioxide were to be produced by first liquefying carbon dioxide near its triple point and then subcooling the carbon dioxide to a solid the carbon dioxide container would have to be a pressure vessel. This is because the triple point for carbon dioxide occurs at a pressure of 3890 torr (75 psi) and a temperature of 216°K. Thus, the carbon dioxide container would have to withstand pressures of at least 5 atmospheres. Since it is doubtful whether a temperature of 216°K could be accurately maintained the container would have to be constructed to withstand considerably more than 5 atmospheres. Also, two cooling systems would be used in the servicing operation, a liquid nitrogen system for solid argon production, and another system for production of a temperature near 216°K for the solid carbon dioxide production.

In order to simplify the servicing techniques investigations were undertaken to determine whether high density solid carbon dioxide could be produced readily directly from the vapor phase. In these experiments it was found that a high density solid carbon dioxide could be grown directly from the gas phase on liquid nitrogen cooled walls of a container with the carbon dioxide gas pressure in the container maintained between 1/4 and 1 atmosphere. This does not mean that outside these pressure limits a high density solid could not be produced, as this was the pressure deposition range investigated. The solid carbon dioxide density achieved in these experiments was 1.65 g/cc at 77°K which compares favorably with the measured density of carbon dioxide of 1.70 obtained under more carefully controlled conditions.[7]

With the demonstration of the successful high density solid carbon dioxide growth directly from the vapor phase this method of production was chosen for the present design. As can be seen in Figure 1 the liquid nitrogen heat exchanger is located in the outer periphery of this container whereas the carbon dioxide inlet manifold is located near the innermost section of the container. This is to prevent the growing solid carbon dioxide from blocking the entrance manifold until the container is nearly full. In practice the warm incoming gas also prevents any blocking of the carbon dioxide inlet system. The liquid nitrogen heat exchanger is thermally isolated by the insertion of mylar tubing between this heat exchanger and other portions of the liquid nitrogen servicing system.

3.4.1 Solid Carbon Dioxide Temperature Control

As was shown in Section 3.1.2 the thermal radiation from the solid carbon dioxide temperature surrounds to the solid argon is the principal heat load on the argon with the exception of the infrared detector heat load. Since the radiative heat load from the solid carbon dioxide temperature surrounds to the solid argon depends on the fourth power of the absolute temperature of the surrounds it is obvious that any substantial reduction in the temperature of the surrounds is extremely beneficial. As can be seen in Figure 4 the solid carbon dioxide temperature attainable and therefore the temperature of the radiative boundary surrounding the solid argon depends on obtaining very low vapor pressure over the solid carbon dioxide. As was shown in Section 3.1.2, the total anticipated thermal loads on the solid carbon dioxide results in a requirement of 8.8 lbs. of solid carbon dioxide which will be vented at a uniform mass flow rate over a period of one year. The pressure of the gas to be vented is simply the equilibrium vapor pressure of the solid carbon dioxide at its equilibrium temperature, and this vapor is vented to zero pressure space conditions. These known conditions plus the known properties of carbon dioxide gas allow the use of the modified form of Poiseuille's equation,

$$\overset{\circ}{m} = \frac{\pi M D^4}{256\, \bar{R}\, \bar{T}\, \bar{\eta}\, L} P^2$$

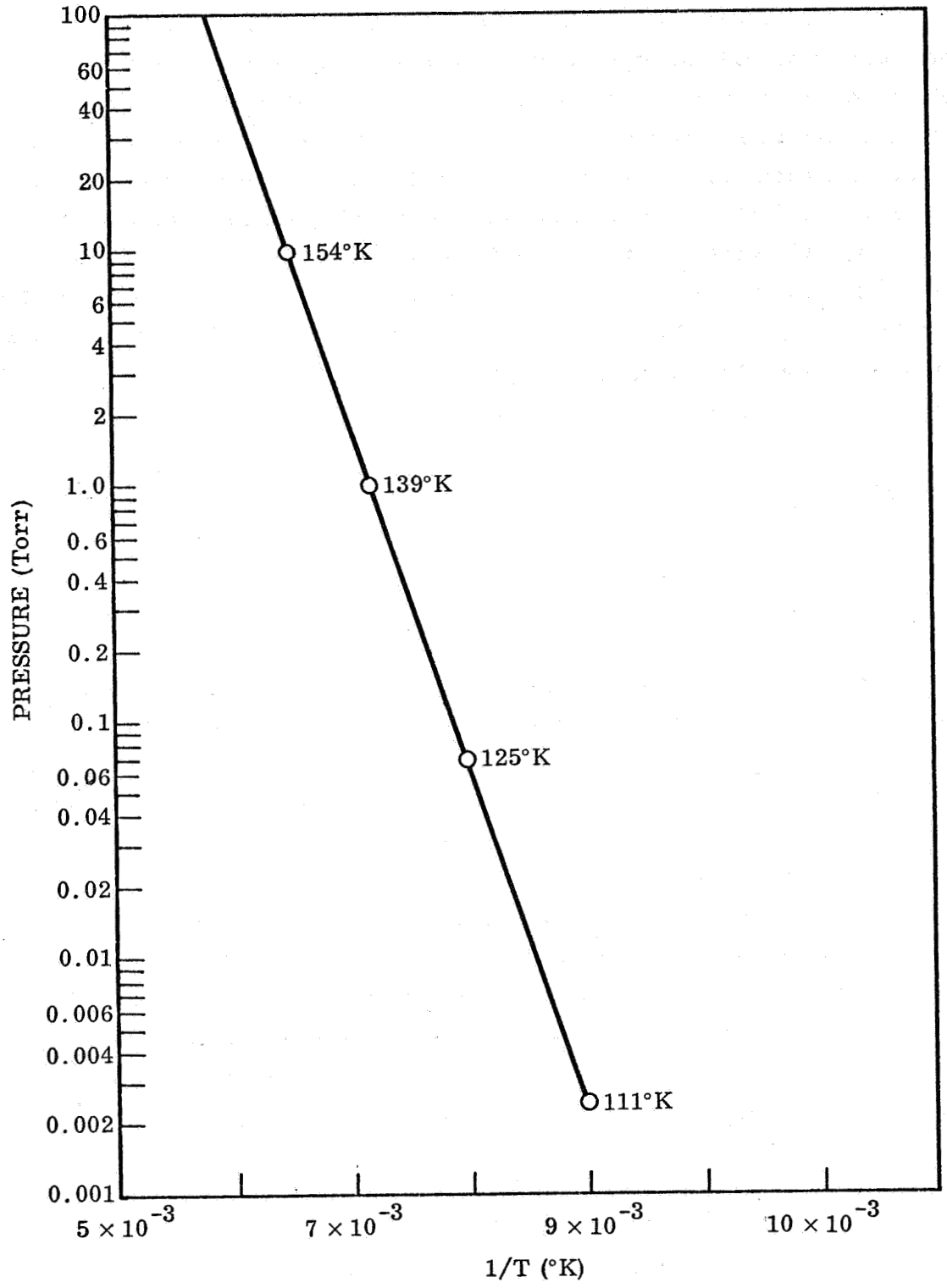

Figure 4. Carbon Dioxide Pressure vs. Temperature

to compute the venting tube diameters and lengths required to maintain a given solid carbon dioxide temperature. Information obtained in this fashion on the attainable solid carbon dioxide temperature as a function of venting tube geometry is presented in Figure 5. Keeping in mind that large venting tube diameters result in large openings in the multilayer insulation blanket with resulting loss in system thermal isolation it is apparent that the venting tube diameter must be limited to below approximately 1/2 inch. In fact, in the present case the carbon dioxide venting tube diameter was chosen to be 3/8 in. This diameter was chosen in order to introduce some clearance between this venting tube and the other fill and vent tubes and the detector rod within the 1.72 in. diameter support column. Since the venting tube length is approximately 8 inches, as can be seen from Figure 5, the anticipated carbon dioxide equilibrium should be 125°K.

3.5 Detector Mounting and Electrical Leads

The mounting surface for the infrared detector consists of a copper cap with a flat upper surface for mounting the detector. The detector would be mounted to this surface with a thin layer of electrical conducting epoxy resin to provide both good electrical and thermal contact. The copper cap for the infrared detector mounting is provided with a short threaded section extending from its bottom surface. Corresponding threads have been tapped in the top of the copper thermal link leading to the argon container. A thin layer of indium metal or vacuum grease applied to the bottom surface of the detector mounting cap ensures good thermal contact between this element and the copper link when the cap is screwed in place. This removable feature for the detector mounting cap provides greater ease for the detector mounting. The use of Evanohm wire for these leads reduces the total heat leak via this path to the argon to below 0.5 mw.

To monitor the carbon dioxide temperature the carbon dioxide container has two separate copper-constantan thermocouples mounted on it. Altogether four leads, two of 3 mil diameter copper and two of 3 mil diameter constantan, are used for these two separate temperature sensors. Two sensors are used only to provide redundance in carbon dioxide temperature measurement capability.

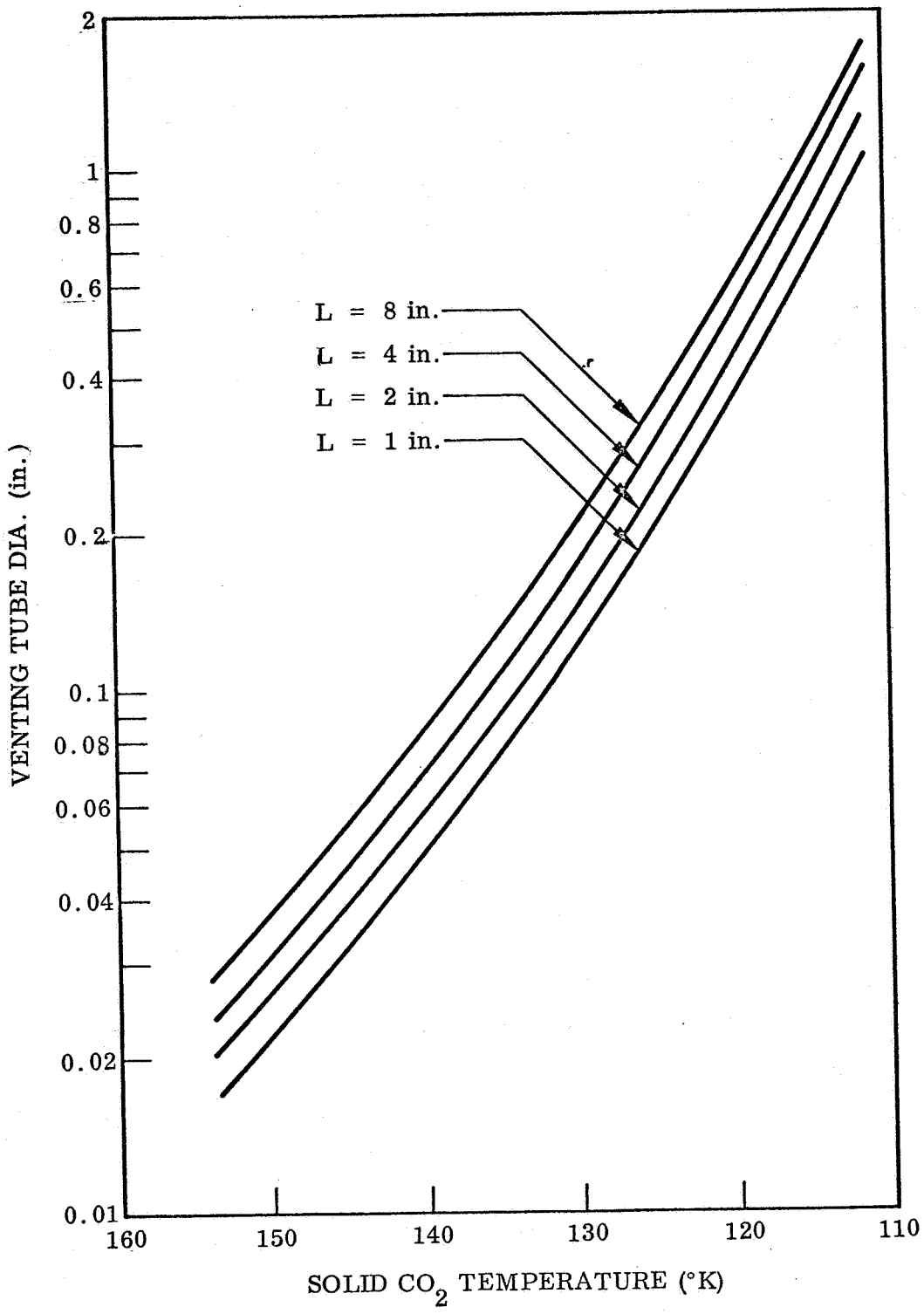

Figure 5. Venting Tube Dai. vs. Solid CO_2 Temperature for Fixed Venting the Tube Lengths (L) Assumed Mass Flow Corresponds to 8.8 lbs of CO_2 Vented in 1 Year's Time

The detector temperature is monitored using a calibrated platinum resistance thermometer. The calibration curve for the resistance thermometer is shown in Figure 6. This platinum resistance thermometer is a Model 118F manufactured by the Rosemont Engineering Co. It is 0.20 inches square by 0.05 inches thick and is bonded to the copper thermal link just below the detector cap mounting point with a thermal conductive epoxy adhesive. A dummy electrical load to simulate the detector heat load is epoxied to the top of the detector mounting cap. The dummy electrical load used is a 20 KΩ carbon resistor. For both the dummy detector load and the platinum resistance thermometer four lead techniques are utilized for the current and voltage measurements. The eight leads to these two elements are "Evanohm" wire 3 mil in diameter by approximately 30 in. long. "Evanohm" wire which is manufactured by the Wilbur B. Driver Co. has a thermal conductivity of 0.152 $\omega/cm^{o}K$ at room temperatures as compared to a thermal conductivity for copper of 4.2 ω/cm^{o} K at the same temperature.

3.6 Refrigerator Service Module

A schematic of the refrigerator service module is shown in Figure 7. The vacuum chamber for the refrigerator is a vertically mounted cylindrical stainless steel container 22 inches long with an internal diameter of 17-1/2 inches. The removable top lid to which the refrigerator is bolted is a 1 inch thick aluminum plate. This plate is provided with four 1/2 inch diameter O-ring seals for the reentrant cryogen fill and vent and liquid nitrogen heat exchanger lines and two 3/4 inch diameter O-ring seals for headers for the feedthroughs for the leads for the thermocouples, platinum resistance thermometer, and the dummy detector load on the refrigerator. Also, in this top plate is a 1 inch diameter O-ring seal for the Irtran II window, a 3/4 inch diameter O-ring seal for an ionization gauge for determining the chamber pressure, plus a high vacuum valve for bleeding the evacuated chamber to air or to 1 atmosphere of helium gas pressure. The vacuum pumping system for this chamber includes a 2 inch water cooled NRC H-2-P Diffusion Pump and 2 inch water cooled chevron baffle, plus a 5 cfm Welch 1402B mechanical vacuump pump. A 2 inch high vacuum gate valve plus a 5/8 inch high vacuum valve on the low pressure side of the

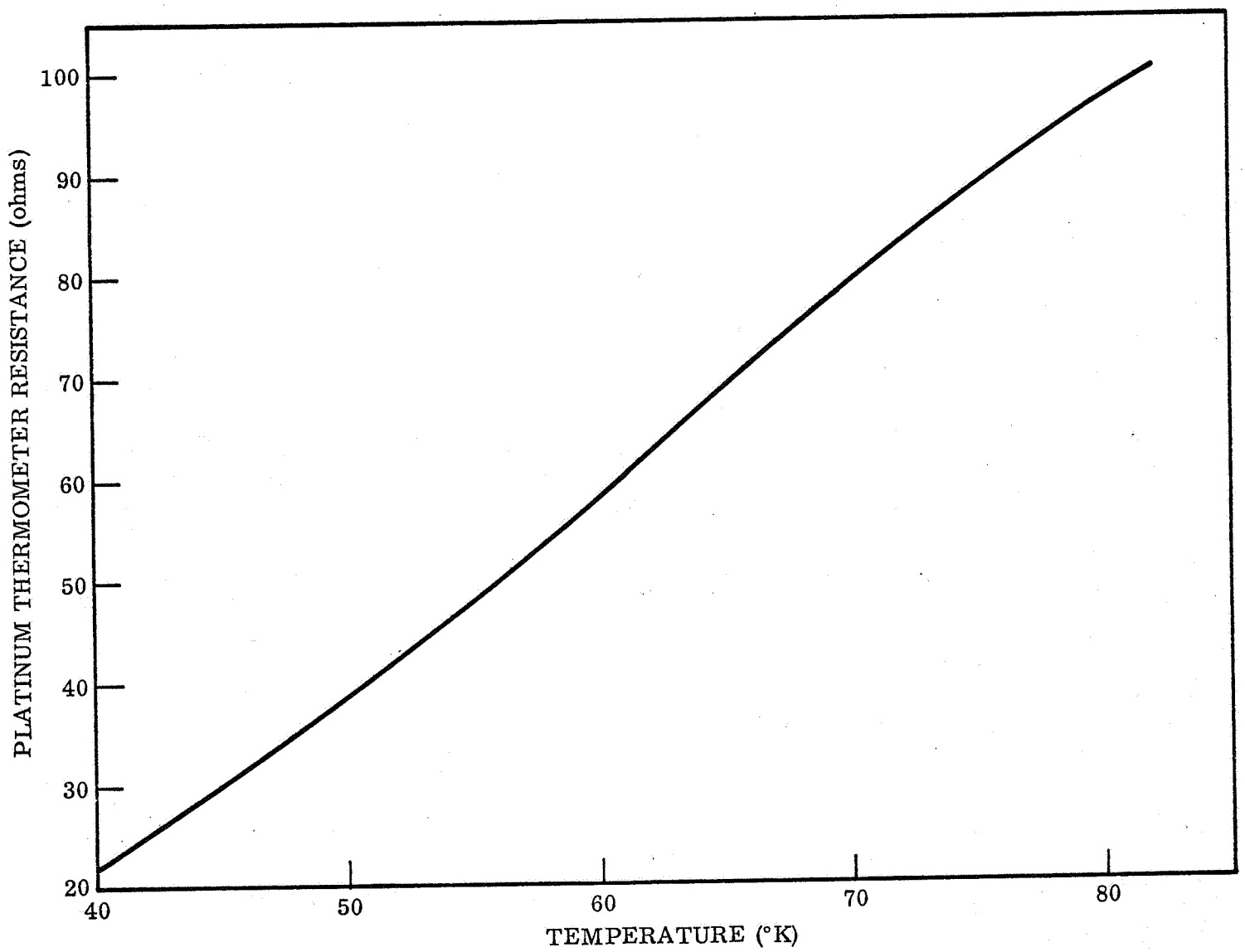

Figure 6. Resistance vs. Temperature for Platinum Resistance Thermometer on Detector Rod

diffusion pump allows this part of the vacuum system to be isolated during mechanical vacuum pump roughdown of the vacuum chamber. A side arm of this high vacuum system shown to the right of Figure 7 is used to evacuate the liquid nitrogen heat exchanger line once the liquid nitrogen cooling operation is terminated. This prevents gaseous heat transfer through the heat exchanger between the carbon dioxide and the warm refrigerator surrounds and between the carbon dioxide and argon.

The carbon dioxide servicing system is shown in the center and lower left-hand portions of Figure 7. Before introduction of carbon dioxide gas, in a container filling operation, the entire manifold system and the carbon dioxide system is evacuated using the Welch 1402B mechanical vacuum pump. Once liquid nitrogen is flowing in the heat exchanger circuit this vacuum pump is isolated from the carbon dioxide manifold and carbon dioxide is introduced into this manifold from the carbon dioxide storage bottle. The carbon dioxide filling pressure is coarsely regulated with the pressure regulator used on the carbon dioxide storage bottle while finer regulation of the container filling pressure is maintained with the throttling valve in the manifold system. The carbon dioxide filling pressure is monitored with a 0 to 30 psia pressure gauge. The total carbon dioxide gas flow at NTP into the carbon dioxide container is monitored using a Precision wet test gas meter. Moisture is removed from the carbon dioxide on the downstream side of the wet test gas meter using a 3 foot long column of calcium carbonate. Complete filling of the carbon dioxide container is indicated by zero gas flow through the wet test gas meter. This condition corresponds to a total measured gas flow through the wet test gas meter of 2,460 ℓ which corresponds to 9.33 lbs. of carbon dioxide in the refrigerator. Partial filling of the container can be controlled to any mass of carbon dioxide by simply terminating the gas flow at a preselected point. After filling has been completed the carbon dioxide storage bottles, wet test gas meter, and drying column are isolated from the carbon dioxide manifold. The wet test gas meter used in the filling operation can then be transferred to the downstream or high pressure side of the mechanical vacuum pump. The high pressure side of the mechanical vacuum pump is provided with a leak tight gas circuit so that the wet test gas meter will measure the total carbon dioxide outflow only. After the transfer of the wet test gas meter has been effected the valve between the vacuum pumping system and the carbon dioxide manifold is opened and pumping on the solid carbon dioxide

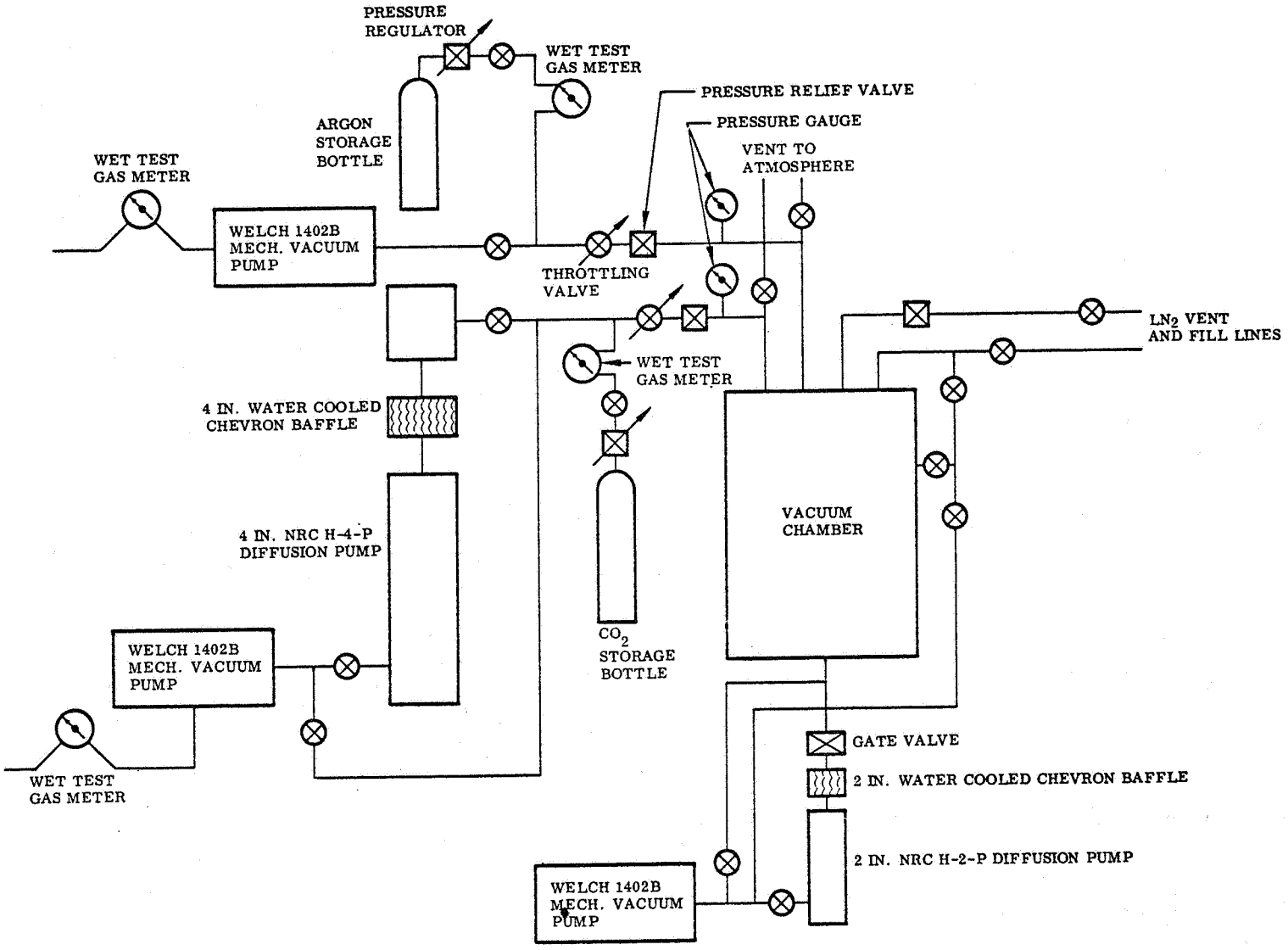

Figure 7 Solid Cryogen Refrigerator Vacuum System

is commenced. For this operation both the mechanical fore pump and a diffusion pump are required.

At 125°K the CO_2 vapor pressure is 3.14×10^{-2} mm Hg. In accordance with the design boil-off at this pressure the pumping speed required is 1.02 ℓ/sec. However, in order to maintain a back pressure approximately 2 orders of magnitude lower than the vapor pressure to simulate the condition of space the required pumping speed at 3.14×10^{-4} mm Hg is 102 l/sec. This pumping speed requirement at such low pressures can't be met with a mechanical pump. The unbaffled pumping speed of the NRC H-4SP diffusion pump below 10^{-3} mm Hg is at 300 l/sec. In conjunction with a chevron baffle the pumping speed is probably reduced to about 200 ℓ/sec. So, this diffusion pumpfore pump system provides the required pumping capacity for maintaining a low carbon dioxide temperature. Ordinarily no carbon dioxide outflow is noted for 15 days as the carbon dioxide temperature is initially about 80°K and the thermal isolation of this system is such that it warms up only about 3°K or less per day. Thus, a period of approximately 15 days passes before the carbon dioxide vapor pressure rises sufficiently for a flow to be noted.

The argon servicing system is shown in the upper left-hand corner of Figure 7. Previous to the filling of the refrigerator container the refrigerator container and argon manifold are evacuated utilizing the mechanical vacuum pump. After both argon and carbon dioxide containers are evacuated with their respective pumping systems; liquid nitrogen transfer into the refrigerator heat exchanger is commenced. Once liquid nitrogen flow is established the vacuum pump is isolated from the argon manifold and argon is introduced in this circuit from the argon storage bottle. As in the case of the carbon dioxide filling system the manifold pressure is coarsely regulated with the pressure regulator used on the argon storage bottle while finer regulation of the argon container is maintained with the throttling valve in the manifold system. The argon filling pressure is maintained above 9.93 psia (514 torr) by monitoring the argon pressure with a 0 to 30 psia pressure gauge. The total argon gas flow at NTP is measured with a Precision wet test gas meter with a calcium carbonate column for drying this gas placed on the downstream side

of the wet test gas meter. Complete filling of the argon container is noted as a no flow condition as measured by the wet test gas meter. This complete fill condition corresponds to a total gas flow through the wet test gas meter of 3,971 ℓ or 14.1 lbs. of argon in the refrigerator argon container. After filling the wet test gas meter can be placed on the downstream or high pressure side of the Welch 1402B mechanical vacuum pump to measure argon boiloff. After the transfer of the wet test gas meter is effected the valve between the vacuum pump and the argon manifold is opened and pumping on the argon is commenced. For solid argon at $50^{\circ}K$ the vapor pressure is 0.15 torr. The argon boiloff at NTP corresponding to an argon lifetime of 1 year is 0.123 cc/sec. The ultimate pressure of the 5 cfm Welch mechanical pump operating at this gas flow rate is $1x10^{-2}$ torr. This constitutes a reasonable downstream pressure although a lower pressure would be somewhat preferable.

4.0 Solid Cryogen Refrigerator Fabrication

The argon and carbon dioxide containers are basically cylindrical structures with wall thicknesses of 0.024 inches and end thicknesses of 0.036 inches. Both containers are constructed from 347 stainless steel rolled sheet stock. The argon container is 8.2 inches in diameter by 5 inches high. Each of the two 0.036 inch thick ends of this container has an identical configured set of 10 holes formed in it. The central hole is for the 1/4 inch diameter copper thermal link to the detector. As can be seen in Figures 8 and 10 there are two uniformly spaced sets of holes concentrically placed about the center hole for tubes to reinforce the container. The inner set of holes are on a 2-3/8 inch diameter circle and the outer set of holes are on a 5-1/2 inch diameter circle. The inner set of holes and alternate holes (three holes) of the outer set of holes are 1/4 inches in diameter and are for 1/4 inch diameter 10 mil wall stainless steel tubes, which are used to reinforce this container. The other three of the six holes on the outer circle are 3/4 inch in diameter and are for 3/4 inch diameter 10 mil wall stainless steel tubes. These tubes serve a dual purpose. They primarily serve as clearance holes for the fiberglas reinforced epoxy support columns for the argon container. Also, these tubes act as reinforcing members for the arbon container. In Figure 8 the headers at the ends of the 3/4 inch diameter support column clearance holes at the bottom of the argon container

can clearly be identified. These headers are inert gas welded to the stainless steel inserts epoxied to the interior walls of the three glass fiber reinforced epoxy columns shown in Figure 12. The edges of the container ends, as well as the edges of the holes through the container ends are rounded approximately 90 degrees. This forms a well defined lip between the tubes, the container outer wall and the container ends so that a good joint is produced for the inert gas welding. The argon container cylindrical outer wall is formed from a single piece of stainless steel sheet whose ends were held butted together; then were tacked together with an electric spot welder, and then were welded together with an inert gas welder to form a welded butt joint. The interior of the argon container with the internal reinforcing tubes, the copper thermal link, and the internal heat exchangers for the thermal link is shown in Figure 9. The internal heat exchanger consists basically of five equally spaced 8 inch diameter pieces of 1/4 inch thick General Electric copper metal foam with a 0.060 pore size. Clearance holes are drilled through these foam metal pieces for the thermal link and reinforcing tubes, and the metal foam pieces are hard soldered to the thermal link and reinforcing tubes. The contact area between the thermal link and the foam metal was increased by soldering strips of 5 mil thick copper foil between the thermal link and foam metal as can be seen in Figure 9. A liquid nitrogen heat exchanger is soldered to the outside of the argon container as can be seen in Figure 8 and 11. This heat exchanger consists of 5 turns of 1/4 inch diameter stainless steel tubing. This heat exchanger was formed by bending the tubing, which was first filled with a low melting point metal alloy Cerrobend to prevent tube wall collapse in the bending operation, about a mandrel with a diameter 1/2 inch less than the diameter of the argon container. The heat exchanger was then spot welded to the outside of the argon container and then hard soldered to the container. The details of the top of the argon container are shown in Figure 11. The thermal link leading to the infrared detector mounting surface is seen extending from the center of the argon container. The platinum resistor for monitoring the detector temperature can be seen epoxied to the side of the thermal link about one third the distance from the detector mounting surface to the top of the argon container. A small stainless steel bellows forms the vacuum seal between the top of the argon container and the thermal link. This bellows takes up any dimensional differences occurring due to thermal

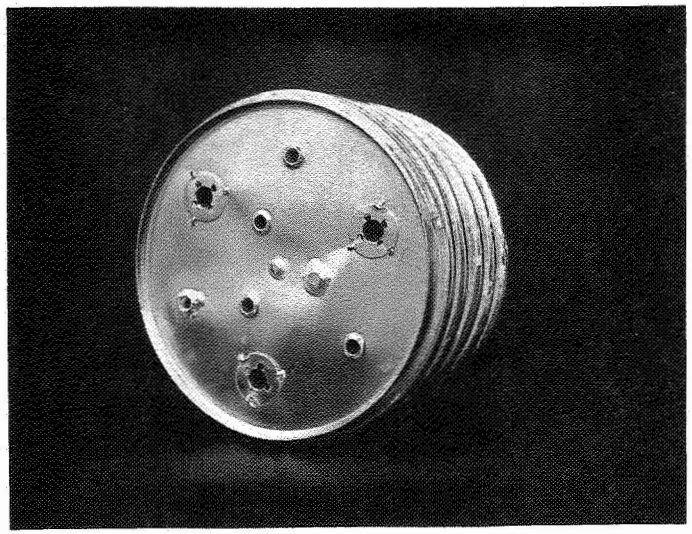

Figure 8. Bottom View of Argon Container

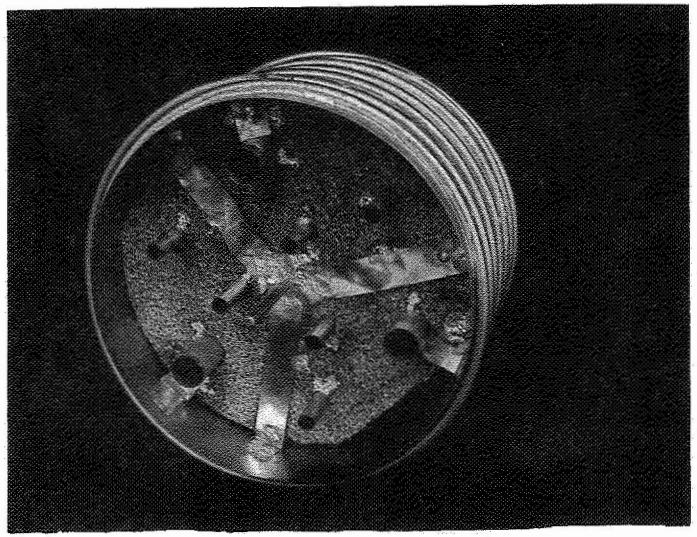

Figure 9. Internal View of Argon Containers

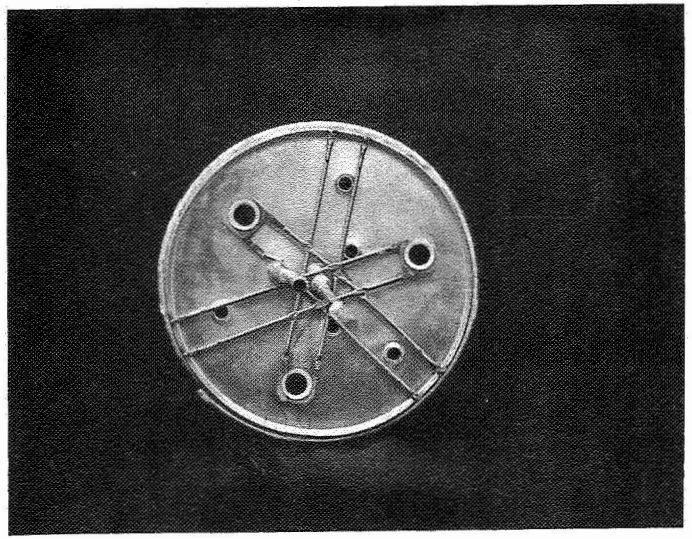

Figure 10. Top View of Argon Container

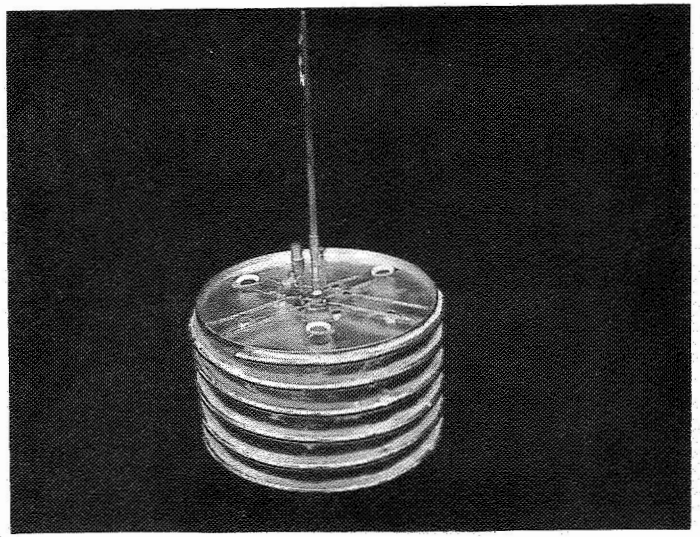

Figure 11. Side View of Argon Container

contraction between the argon container and the portion of thermal link internal to the argon container during the cooling of the refrigerator. The argon fill and vent tube entrance is a 3/8 inch diameter tube which can be seen projecting from the top of the argon container to the left of the thermal link in Figure 11.

After the completion of the argon container system, the entire assembly was gold plated to reduce the absorbtance of the container outer surface for infrared radiation. The completed argon container was vacuum leak tested using helium mass spectrometer leak detector techniques before and after the gold plating process.

The restraining system for preventing excursion of the argon container under lateral loads is clearly shown in Figures 10 and 11. This system engages the fiberglas reinforced epoxy columns, which extend from the carbon dioxide container in order to support the argon container, near the top of these columns in the vicinity of the carbon dioxide container, only when lateral loads are present. This system of restraining bars thus couples the two containers together under lateral loads, causing the entire refrigerator assembly suspended from the main refrigerator support column to move as a unit.

The carbon dioxide container is shown in Figures 12, 13, and 14. This container is annular with an inner diameter of 3 inches, an outer diameter of 9.2 inches, and a height of 4.25 inches. The inner diameter provides a hole of sufficient diameter for the clearance of the main support column for the refrigerator. This container is reinforced with six 1/4 inch diameter 10 mil wall stainless tubes equally spaced on a 6-1/4 inch diameter circle. Additionally, on the bottom end of the carbon dioxide container there are three 1/2 inch diameter holes equally spaced on a 4-inch diameter circle for the carbon dioxide gas fill manifold. The container and liquid nitrogen heat exchanger fabrication techniques for the carbon dioxide container are identical to those used in the argon container manufacture. The carbon dioxide gas manifold was constructed by taking three 1/2 inch diameter to 3/8 inch diameter reducer fittings with a 3/4 inch hexagonal nut at one end and boring out a central hole in the fittings to 0.377 inches. Next the gas injection system internal to the carbon dioxide container was fashioned by taking 3 sections of 3/8 inch diameter 10 mil wall stainless

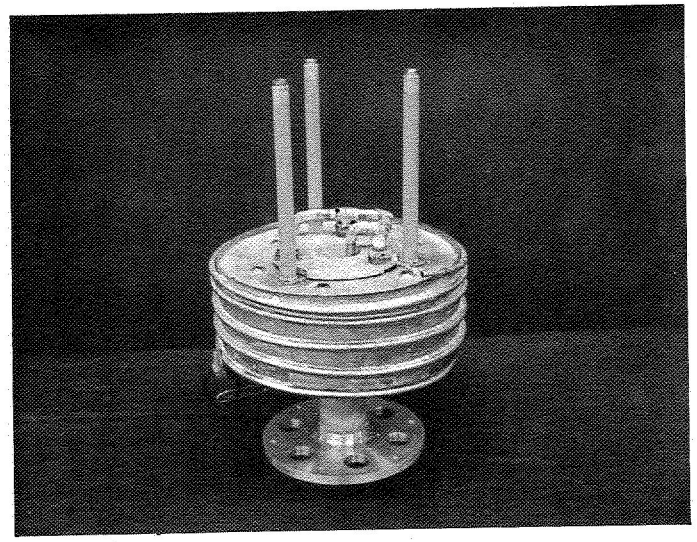

Figure 12. Side View of Carbon Dioxide Container

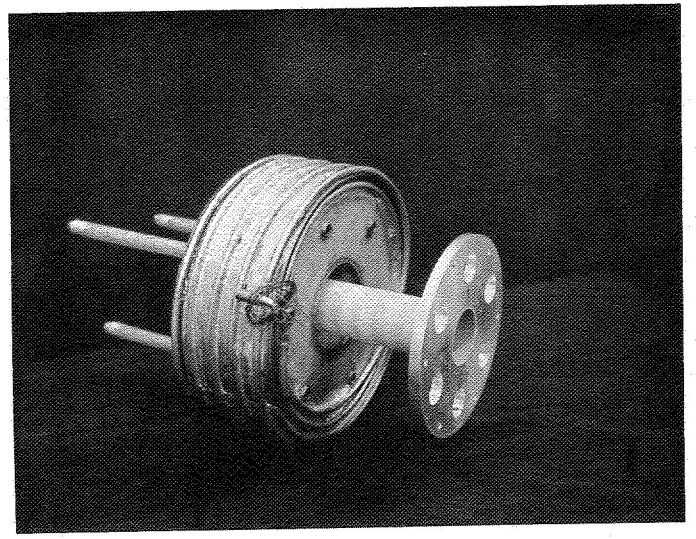

Figure 13. Top View of Carbon Dioxide Container

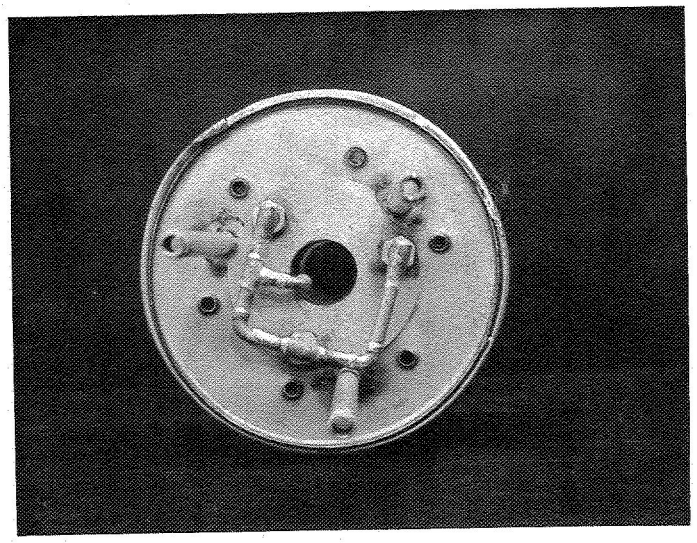

Figure 14. Bottom View of Carbon Dioxide Container

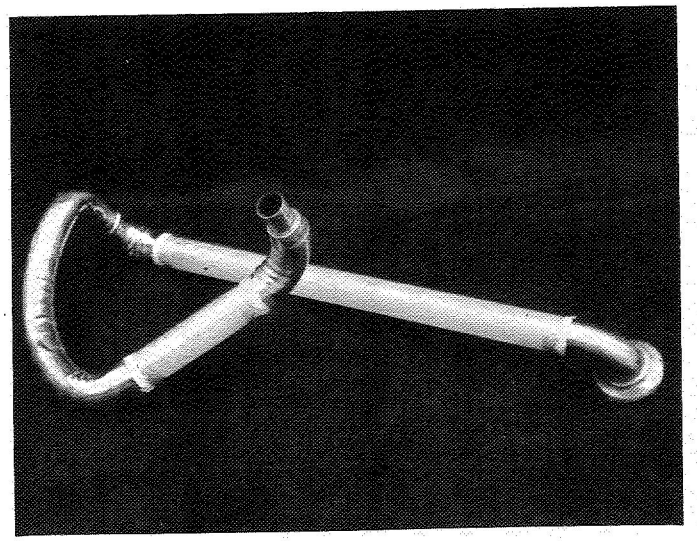

Figure 15. Argon Vent Tube System

steel tubing sealed at one end and slitting a number of openings in the walls of each tube. Then the open end of each tube was hard soldered into a modified reducer at the hexagonal nut end. Next these elements were inserted into the 1/2 inch diameter holes at the bottom of the carbon dioxide container with the hexagonal nut on the interior of the container and the 1/2 inch diameter threaded section jutting out of the container and sealed in place with hard solder applied to the interior side of the container end plate. The carbon dioxide container has three 1/4 inch thick equally spaced expanded copper foam metal heat exchangers hard soldered to its interior walls. These foam metal heat exchangers are provided with clearance holes for the carbon dioxide gas fill and vent manifold.

The bottom container end plate is inert gas welded to the rest of the container to complete the carbon dioxide container assembly. The threaded reducer section on the carbon dioxide manifold serves the dual function of inlet and vent tubes for the carbon dioxide gas and mounting studs for the flange for the main support column for the refrigerator. The aluminum mounting flange for the main support column is 5 inches in diameter by 1/4 of an inch thick. The main support column is epoxied to the interior surface of a thru hole in the center of this flange. After the flange for the support column has been bolted to the carbon dioxide container the exterior sections of the carbon dioxide manifold system is hard soldered in place. This assembly is shown clearly in Figure 12. After completion of the carbon dioxide container and carbon dioxide manifold system this entire assembly was vacuum leak tested using helium mass spectrometer leak detection techniques. The support column flange has three equally spaced recessed sections on its outer edge for clearance of the argon container support columns. These columns are epoxied to headers identical to those used on the argon container, which are then inert gas welded to the bottom of the carbon dioxide container at equally spaced points on a 5 1/2 inch diameter circle. The positions of the support columns correspond to the recessed portions of the support flange. These columns are 7 inches long and have external and internal diameters of 0.560 and 0.512 inches respectively. Complete details of this arrangement are shown in Figures 12 and 14. The main support flange for the refrigerator is epoxied to the top of the refrigerator support column. This aluminum flange is 6-1/2 inches in diameter by 3/8 inches thick. Both this flange and the 5-inch diameter flange at the bottom of the support column,

which fastens to the carbon dioxide container, are provided with a 1/8 inch wide raised shoulder so that the total length of the epoxy bond between the support column and the flanges is 1 inch. The top flange is provided with six 0.261 inch diameter clearance holes equally spaced on a 5-3/4 inch diameter circle for mounting the refrigerator to the top plate of the vacuum chamber. The stainless steel and mylar tubing system shown in Figure 15, which is a section of the argon fill and vent line, is soldered to the top of the argon container as is shown in Figure 1. Vertical sections of 3/8 inch I.D. mylar tubing 7 inches long are epoxied to the argon and carbon dioxide fill and vent systems. These mylar tubes communicated from the interior of the refrigerator up the inside of the main support column as indicated in Figure 1. The headers at the bottom of the argon can are next inert gas welded to the stainless steel sleeves at the ends of the three glass fiber reinforced epoxy columns which extend from the bottom of the argon container. Then the stainless steel and mylar tubing sections completing the liquid nitrogen circulation circuit for the internal heat exchangers are soldered in place and 7 inch lengths of 1/4 inch I.D. mylar tubing are used to bring the lines for the liquid nitrogen circulation system up the interior of the main support column. The framework used to support the multilayer insulation system approximately 1 inch away from the argon container is shown in Figure 16. This framework is constructed from 1/16 inch diameter stainless steel tubing having a 10 mil wall thickness. The individual sections of the framework are bonded together using inert gas welding techniques. A single layer of 1.5 mil copper foil completely covers the exterior of this framework and is used to provide a solid carbon dioxide temperature shroud for the argon container. Both this framework and the copper foil covering are firmly soldered to the exterior of the carbon dioxide container both to support the framework and to provide good thermal contact between the copper foil and the solid carbon dioxide. This system is shown in Figure 18. As previously indicated in the discussions of the refrigerator thermal design a floating radiation shield is located between this framework and the argon container. Structural rigidity in the floating radiation shield is accomplished by also supporting it with a framework of 1/16 inch diameter stainless steel tubing. This framework is indicated in Figure 17. Again, the floating radiation shield supported from this framework is constructed from pieces of 1.5 mil thick copper foil which are bonded together and also to the framework using soft solder. Openings are provided

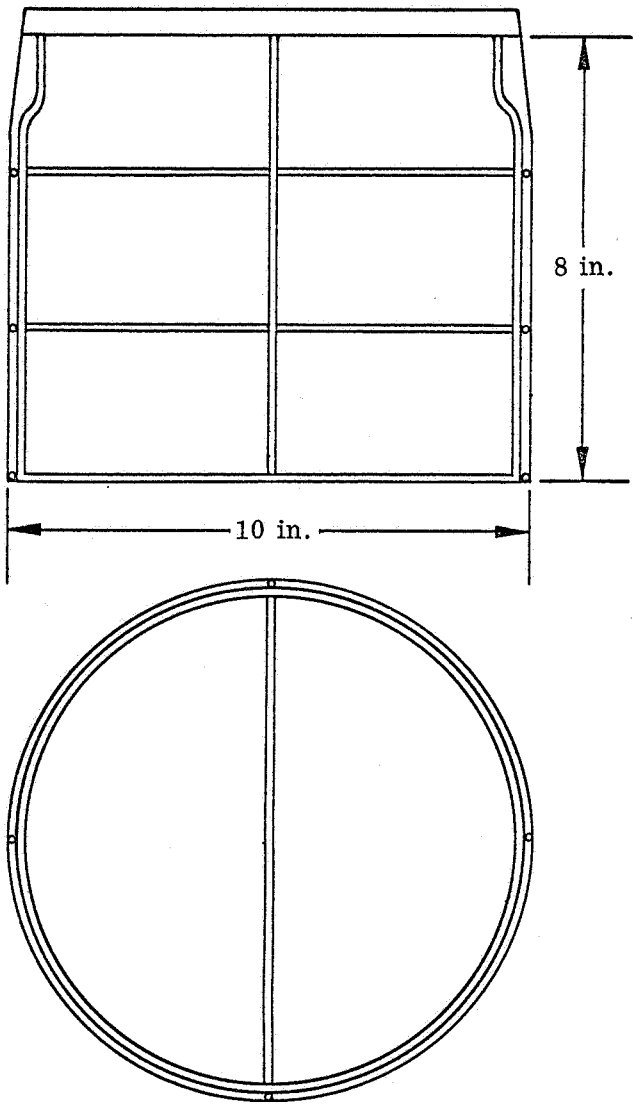

Figure 16 Support Cage for Multilayer Insulation

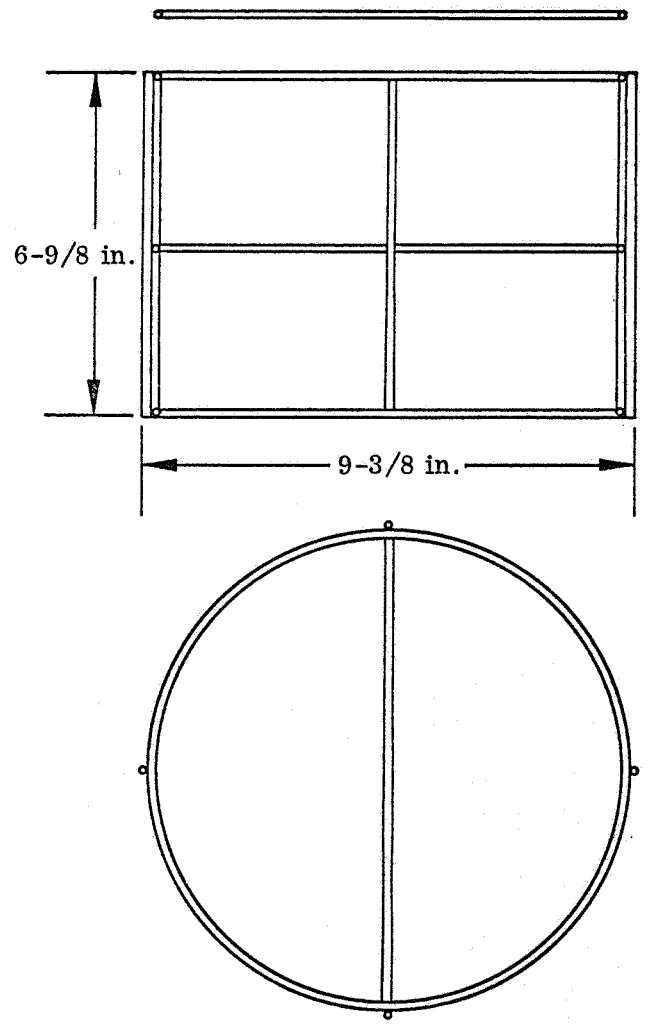

Figure 17 Support Cage for Floating Radiation Shield

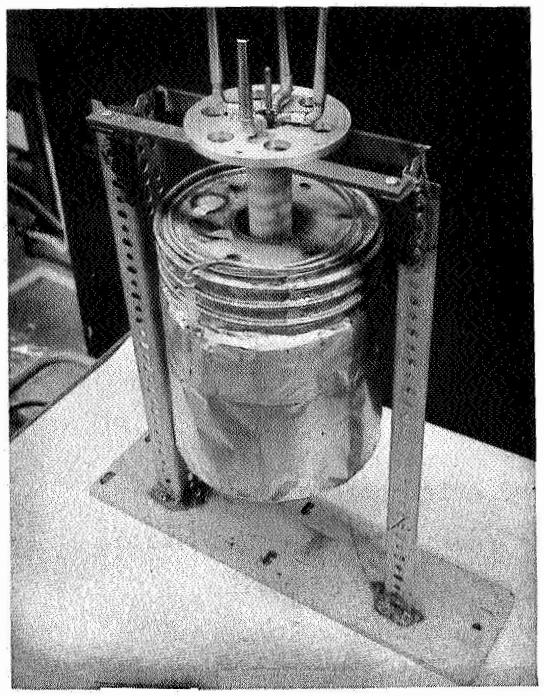

Figure 18 Top View Uninsulated Refrigerator Assembly

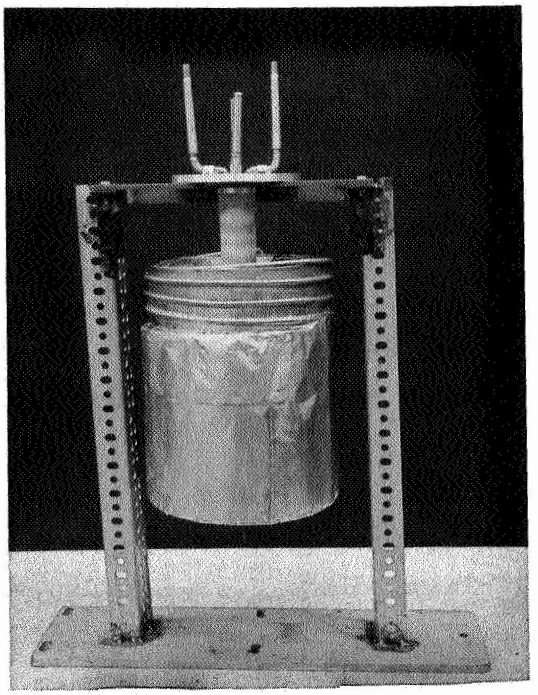

Figure 19 Side View Refrigerator Assembly

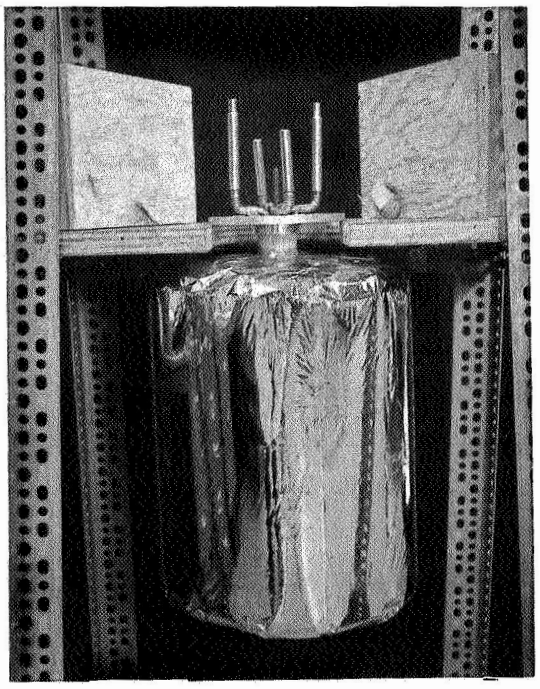

Figure 20 Side View Insulated Refrigerator Assembly

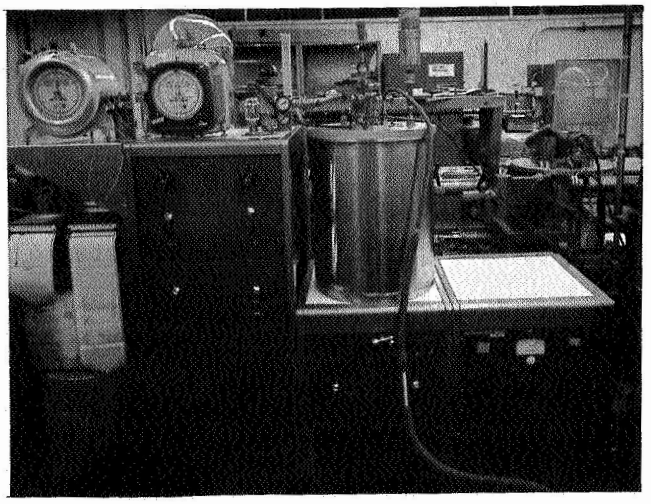

Figure 21 Refrigerator Service Module

in this floating radiation shield for the argon container support columns, argon fill and vent line, the thermal link to the detector, and the liquid nitrogen heat exchanger lines. This floating radiation shield is held in place between outer shroud and the argon container with a system of nylon thread supports. Vibration suppressors made of teflon are attached to the shroud and radiation shield framework. These vibration suppressors are designed to contact the container under lateral accelerations. After completion of the refrigerator assembly and before application of a multilayer insulation blanket about the refrigerator, the entire refrigerator was leak tested using helium mass spectrometer leak detection techniques.

The multilayer insulation system was then applied after the foregoing refrigerator construction phases had been completed. A 1/4 inch wide zone of intermediary, i.e., Dexiglas*, insulation was provided between the refrigerator insulation penetration, i.e., the main support column, and the multilayer insulation system. This intermediary insulation zone is obtained by spirally wrapping a 1/4 inch thickness of Dexiglas about the glass filament wound epoxy reinforced refrigerator support column between the top of the carbon dioxide container and the top of the column.

This spiral covering of Dexiglas paper was wrapped loosely to reduce solid phase thermal conduction between the refrigerator support column and the edge multilayer insulation system; approximately 12 layers of Dexiglas were used for the 1/4 inch intermediary insulation layer. The annulus between the 3 inch diameter center hole in the carbon dioxide can and the 1.86 in. diameter refrigerator support column was insulated with approximately 20 layers of double aluminized mylar-Tissuglas† insulation having a width equal to the height of the carbon dioxide container. The multilayer insulation system for the refrigerator exterior is applied by spirally wrapping 150 layers of double aluminized mylar radiation shields with Tissuglas spacers in a two inch thick blanket about the outside of the refrigerator. This blanket is applied using a continuous length of insulation and the ends of the 36 inch width of insulation applied overhang to the top of the carbon dioxide container and the bottom of the argon container equally.

*Manufactured by the Dexter Paper Co.

†Manufactured by the American Machine & Foundry Co.

The ends of the insulation system are applied over the top of the carbon dioxide container and the bottom of the argon container using a displaced gore application technique. In this technique the overhanging ends of the insulation layers are taken ten at a time starting with the innermost layers. Triangular sections are cut out of these overhanging insulation layers so that the apex of the triangular cuts terminates at the refrigerator top or bottom depending on whether the overhanging layer in question is at the refrigerator top or bottom. The edges of the overhanging insulation layers are serrated in this process so that when they are folded over on the top of bottom of the refrigerator they butt nicely along their edges leaving no gap. The ends of the triangular serrations in the insulation edges at the top of the refrigeration are truncated approximately 1 inch back from their vertex so the ends will conform to the Dexiglas covered main support column. After the serrated insulation layers have been folded down their top edges are taped together with small pieces of adhesive backed mylar tape. After each 10 layers of the serrated insulation ends have been taped across the top or bottom of the refrigerator they are covered with a disk of Tissuglas paper. This provides a smooth surface for the next set of layers. The serrations in the next set of layers are displaced so that any gaps along the edges of the serrations in these layers will not view gaps in the former insulation layers. This displaced gore technique prevents relatively hot insulation layers from viewing cold insulation layers, and thereby results in a significant improvement in multilayer insulation system performance. At the top of the refrigerator the electrical leads from the thermocouples, the platinum resistance thermometer, and the dummy infrared detector load resistor are worked out from the interior of the refrigerator through the gores of the insulation. This serves to thermally ground these leads to the various layers in the insulation, and thereby reduce heat leaks to the cryogens via these leads. This is because thermal energy added to reflecting shields in the insulation systems tends to be rejected from the insulation blanket. The radiation heat flow encounters less resistance in flowing out of the insulation than in flowing toward colder insulation layers.

After the insulation wrap is completed the area of the wrap about the penetration is covered with approximately a 1-inch thickness of 5 inch diameter

Tissuglas disks. The disks have approximately a 1-3/4 inch diameter center hole so that they fit tightly on the fiberglas support tube. These disks serve to protect the penetration area from radiation from the refrigerator surrounds.

After the multilayer insulation blanket on the refrigerator was completed the insulation of the interior of the main support column was initiated. Since any insulation in the neck tube area blocks the most direct path for evacuating the interior of the refrigerator, two 3/8 inch diameter mylar tubes are inserted into the neck tube having sufficient length to penetrate through the subsequently applied neck tube insulation system to provide a high conductance between the evacuated volume about the argon container and the vacuum environment exterior to the refrigerator. In this system the neck tube is simply filled with 3-inch thick layer Dexiglas insulation which has been cut into small pieces approximately 1/4 inch on a side. This step completes the basic assembly of the solid cryogen refrigerator. The completed system shown in Figure 20.

5.0 Solid Cryogen Refrigerator Characteristics Tests

5.1 Solid Cryogen Refrigerator Thermal Characteristics Tests

For thermal testing the refrigerator is mounted in the vacuum chamber on its serving unit and the vacuum chamber is evacuated to a pressure of approximately 5×10^{-5} torr. This system is shown in Figure 21. Since the multilayer insulation system on the refrigerator has a rather low gaseous conductance and also outgasses rather vigorously the initial pumpdown of the refrigerator takes from 12 to 24 hours. This pumpdown time appears to depend strongly on the amount of water vapor which has been absorbed by the insulation system. Once a low vacuum chamber pressure has been obtained, and the argon and carbon dioxide containers have been evacuated, then liquid nitrogen circulation through the refrigerator heat exchangers is commended.

Fill tests carried out with the refrigerator indicate that using the cryogen filling techniques discussed in Section 3.6, on the refrigerator servicing module, a complete filling operation results in a mass of 14.1 lbs. of argon

and 9.33 lbs. of carbon dioxide in the refrigerator. Using the measured volumes of 3770 cc and 2613 cc for the argon and carbon dioxide containers respectively the density of the solid cryogens obtained in the refrigerator are respectively 1.695 g/cc and 1.655 g/cc or respectively 99.7 and 97.3 per cent of the accepted maximum densities of argon and carbon dioxide at liquid nitrogen temperature. The container volumes were determined by measuring the weight and thereby the volume of water required to completely fill the containers. The corresponding volumes of argon and carbon dioxide metered into the refrigerator in a complete filling operation are 3,971 ℓ and 2,460 ℓ respectively. The time required for the basic filling operation is approximately 4 hours.

The initial tests on the thermal performance or cooling lifetime of the solid cryogen refrigerator system were quite disappointing. In these tests the insulation blanket used on the refrigerator was a layer of approximately 160 layers of a double aluminized mylar-Dexiglas insulation applied in a blanket approximately 2 inches thick. The results of these tests can be summarized simply as follows. With both argon and carbon dioxide containers full, and these cryogens at their operating temperatures, the heat loads on the cryogens determined from the cryogen boiloff rates were 92.5 and 235 milliwatts respectively. With the argon container empty and the carbon dioxide container filled with carbon dioxide at operational temperature the argon container remained at the carbon dioxide temperature and the total heat leak to the carbon dioxide was 318 milliwatts. This heat leak approximated very closely the total heat leak to both containers in the first test 327.5 milliwatts. Since the total heat leak in both cases is the same and the empty argon container remained at the carbon dioxide temperature the low carbon dioxide boiloff in the first test was actually due to a strong thermal coupling between the two cryogen containers. The argon was being expended in cooling the carbon dioxide. Also, since the total heat leak into the refrigerator was three times that predicted in the thermal design the thermal performance initial aluminized mylar-Dexiglas insulation wrap was quite poor. There are two explanations for the poor insulation thermal conductivity value achieved. First, it was determined from post-test measurements of the emittance of the aluminized mylar radiation shield material used in the above tests that the material had an emittance varying from .055 to .06

whereas the emittance of good samples of aluminized mylar should be .03. This higher emittance value would increase the heat flow through a multilayer insulation system by 25 per cent. Second, there is some evidence that the insulation wrap had a higher layer density than the optimum value. This would lead to even more severe problems were the edges of the insulation gores folded over since here the insulation tends to be locally compressed. As can be seen from Figure 22 the multilayer insulation thermal conductivity for a double aluminized mylar-Dexiglas insulation system rises quite rapidly with increasing layer density.

As a result of the above tests it was clear that first the mode of strong thermal coupling between the argon and carbon dioxide containers had to be determined and removed, and second, the thermal effectiveness of the multilayer insulation wrap needed to be significantly improved. It was obvious from the degree of thermal coupling between the argon and carbon dioxide containers that a conductive heat path was involved. Simple calculations indicated that neither radiation or residual gas heat transfer could account for the heat fluxes involved. Upon removing the insulation and radiation shields from the refrigerator it was observed that the metal section of the argon container fill line slightly above where it emerges from the argon container was in contact with the main refrigerator support flange located at the bottom of the argon container. Another potential source of heat transfer into the argon container was through the LN_2 heat exchanger line. It appeared possible that thermal contraction during cool down could cause the LN_2 line going directly from the neck section to the argon container to come into contact with the CO_2 manifold. This would result in an effective heat transfer path of only approximately 3 inches for the 1/4 inch O.D. 10 mil wall stainless steel LN_2 line. If the contact were perfect it would be possible to transfer some 46 milliwatts into the argon container. The argon and liquid nitrogen heat exchanger lines were therefore redesigned in order to improve the clearances between these lines and the refrigerator components and also to reduce their thermal conductivity. This redesigned system is the system described in Section 4.0 in the description of the refrigerator fabrication. However, an emphasis of the attributes of the present system are in order here. The 3/8 inch nominal

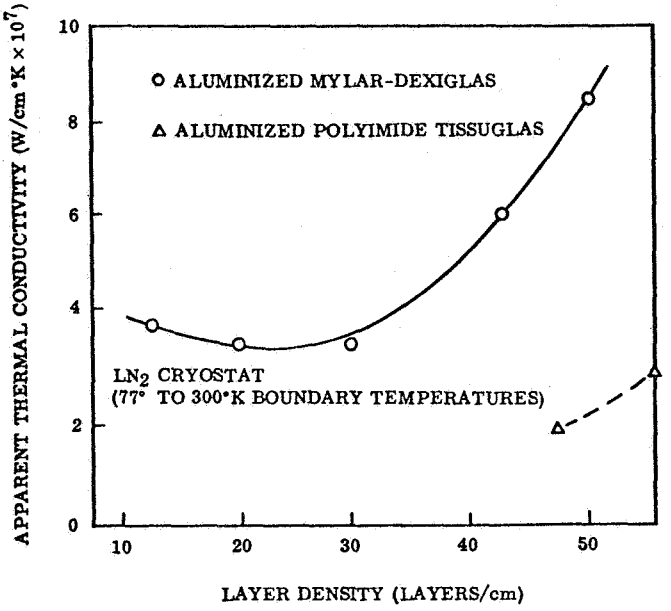

Figure 22 Thermal Performance of Double-Aluminized Mylar and Dexiglas Multilayer System and Double-Aluminized Polyimide and Tissuglas Multilayer System Versus Density

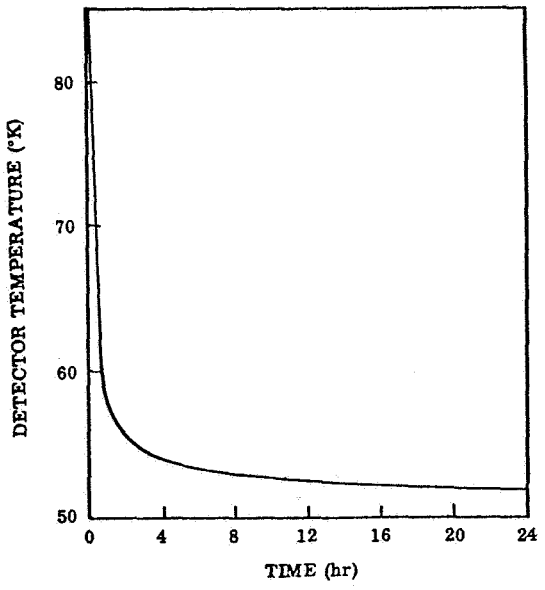

Figure 23 Detector Temperature vs. Time. Time origin referred to commencement of pumping on argon.

diameter mylar argon fill and vent tube coming down the main support column makes a transition to a 1/2 inch diameter stainless steel tubing. This tubing section then makes a 90° bend and passes between the argon and carbon dioxide containers above the floating radiation shield to the outer edge of the carbon dioxide container. At this point this section makes a 180° turn and passes beneath the radiation shield parallel to the argon container more than half-way across the container to the point where it turns 90° and is joined to the container. The straight sections of this tubing both above and below the radiation shield are made of mylar to reduce the solid phase heat transport along this tubing. The liquid nitrogen heat exchanger line was rerouted with sufficient clearance so that thermal shorts could not develop between the argon and carbon dioxide containers. Extra mylar sections were also added in these liquid nitrogen lines to further reduce solid phase heat transfer along these lines between containers.

In this reconstruction the refrigerator was insulated with a two inch insulation thickness consisting of 150 layers of a newly developed LMSC high performance multilayer insulation applied in a two-inch thick blanket. This improved insulation system utilizes Tissuglas* a 0.6 mil thick submicron-size unbonded borosilicate glass fiber mat material which is similar to the Dexiglas radiation shield spacer material used in the earlier refrigerator insulation wraps, except for the greater thickness (2.8 mils) of the Dexiglas sheets. This means that at an equivalent radiation shield density (shields/in), that the interlayer contact resistance or solid conduction term should be decreased over the Dexiglas case with the application of Tissuglas spacer material due to the lower "compression" of the insulation system. This is supported by the cryostat data on the thermal conductivity of the two systems shown in Figure 22. Also, the thermal conductivity of this insulation system is not as sensitive a function of layer density as the double aluminized mylar-Dexiglas insulation system. Thus, the thermal conductivity of this insulation system should not be as sensitive to local compressions in the fold areas of the insulation gores. As will be seen the excellent thermal performance of this insulation system were borne out in the refrigerator thermal tests.

*Manufactured by the American Machine & Foundry Co.

Upon completion of these modifications the refrigerator partially filled with 2060 g of carbon dioxide (4.54 lbs) and 3050 g of argon (6.74 lbs). This corresponds to the refrigerator being approximately 50 per cent charged with respect to its total carbon dioxide and argon capactiy. The partial fill was made so that the characteristics over a filling lifetime of the refrigerator could more readily be evaluated, in a reasonable period of time. After the filling operation had been completed, a cooling period of approximately 4 hours, using a continued liquid nitrogen flow, was required to cool the entire mass of solid argon down to liquid nitrogen temperature. When subcooling of the solid argon to liquid nitrogen temperature had been completed the liquid nitrogen flow through the internal heat exchanger was terminated and this system was evacuated. This latter step prevents thermal contact between the solid argon and solid carbon dioxide via gases trapped in the nitrogen heat exchanger system.

Direct pumping of the argon was thence commenced utilizing the 5 cfm mechanical vacuum pump in the refrigerator servicing module. In Figure 23 the argon cooling curve is indicated, with the time origin referred to the initial beginning of the argon vapor pumping operation. Approximately 24 hours were required to reach steady state temperature conditions (51.9^{o}K). But within 4 hours after the initiation of the pumping operation the detector temperature was within 2°K of its final operating temperature. A 20°K Ω carbon resistor fastened with an epoxy adhesive to the infrared detector serves as the dummy detector heat load. The electrical power dissipated in this element is determined by using standard 4 wire techniques and a Leeds & Northrup K-3 potentiometer for the current and voltage determinations. With no electrical power dissipation in this dummy detector load, the argon boiloff at NTP is 0.135 cc/sec which corresponds to a total heat load on the argon of 44.8 mw. 15.7 mw of this total heat load is radiation from the refrigerator surrounds. This was determined by cooling a 1 inch diameter copper disk which was located just over the top of the detector mount to 200°K using cold circulating nitrogen gas. With this cooled disk in place the heat load on the argon was reduced to 29.1 mw. The original heat load predicted on the basis of the refrigerator thermal design from the immediate surrounds of the argon container was 15 mw, so that larger heat leaks to the argon container were experienced than had

originally been predicted. It should be indicated, for example, if a poor gold plating operation had been done on the argon container so that its emissivity was 0.05 this would account for the additional heat leak. An analysis was made of the argon boiloff as a function of the temperature of the carbon dioxide during the time period when the carbon dioxide was warming up from a temperature of $80^{\circ}K$ to its final operating temperature of $129^{\circ}K$. The analysis indicates that approximately 19.2 mw of radiative heat transfer exists between the carbon dioxide and argon containers at the carbon dioxide operating temperature. The additional 9.2 mw of radiant heat transfer over the design goal (see Table 1) accounts for most of the additional observed heat transfer to the argon container. This additional heat transfer could undoubtedly be eliminated with more care in the gold plating operation and if the liquid nitrogen heat exchanger geometry on the outside of the argon container were changed to eliminate interreflection of radation. These interreflections result in increased absorption of incident thermal radiation.

In terms of the original design goal of 25 mw of detector heat load (15 mw of I^2R heating plus 10 mw of radiation load) and for the originally planned mass of solid argon (13.7 lbs) the solid argon lifetime would be 8 months. Using the maximum mass of argon that the refrigerator will hold (14.4 lbs) a total detector heat load of 17.6 mw could be sustained. Although with the present refrigerator system located in its vacuum chamber the radiant heat load on the detector from the surrounding hohlraum cavity contributes 15.7 mw for a properly designed telescope system,this heat load would be below 5 mw and the allowable detector bias current electrical power dissipation would be above 11 mw.

Carbon dioxide boiloff was not observed until the 15th day after the filling of the refrigerator. During this time the solid carbon dioxide temperature rose from approximately $80^{\circ}K$ to its final equilibrium temperature of $129^{\circ}K$. This final carbon dioxide equilibrium temperature is $4^{\circ}K$ higher than the original $125^{\circ}K$ design goal. The carbon dioxide boiloff under equilibrium conditions is 0.069 cc/sec which corresponds almost exactly to a one year lifetime for the original design goal of 8.8 lbs of solid

carbon dioxide for 1 year's operation. The total heat load to the carbon dioxide under these conditions is 75 mw.

Several experiments have been performed on the degree of detector temperature regulation under varying detector heat loads. A careful analysis of this data indicates that the change in detector temperature will be .028°K/mw under varying heat loads. This latter temperature regulation agrees well with the originally predicted detector regulation. It should be noted, however, that this data was taken under conditions in which there is good thermal contact between the solid argon and the detector heat exchanger located in the argon volume. In order to investigate the thermal performance of the argon system near the end of the argon cooling lifetime the electrical heat load to the argon was increased to 240 mw until only 0.5 lbs of argon remained. This corresponds to 3.65 per cent of a complete argon fill (13.7 lbs) remaining. A detector I^2R heating load of 25 mw was then re-established. Under these conditions the detector operating temperature was 52.6^{o}K compared to the original value of 51.9^{o}K. Also, the detector temperature regulation under varying thermal loads under these conditions was determined to be 0.037^{o}K/mw.

5.2 Solid Cryogen Refrigerator Mechanical Characteristics Tests

As has been previously discussed a filament wound fiberglas epoxy reinforced support column identical to the column used in the present refrigerator unit was tested for its structural strength characteristics under static test conditions. The main support column is the most critical refrigerator element from a structural point of view. Tests performed on this sample support column indicated that with the column design chosen the column strength is sufficient to meet the required column tensile and shear loads which correspond to acceleration of the total refrigerator mass of 30 g's parallel to the column and 10 g's lateral to the column. However, in compression the column would support only the equivalent of a 15 g acceleration of the refrigerator. As was discussed in Section 3.1.1, however, it is felt on the basis of the reported tensile strength of filament wound epoxy impregnated materials that the failure in the present sample column in tension was due to structural

imperfections. Thus, a quality assurance program should result in columns having the same dimensions as those used in the present refrigerator unit meeting the criterion of being able to support a load equivalent to a 30 g acceleration of the mass of present refrigerator in compression.

In order to define the magnitude of the accelerations the present unit should have to withstand a 1 g low level resonant survey over the frequency range 35 cps to 3000 cps was performed. The refrigerator containers were filled with gelatin and loaded on the outside with a uniform weight distribution of sheet lead to simulate the cryogen and insulation weights. The refrigerator was mounted horizontally to the head of a Calidyne shake table with a 90° angle 1 inch thick aluminum frame which was bolted and welded to form a rigid structure. A 0 to 10 g Endevco accelerometer was mounted with its axis normal to the axis of the refrigerator (normal to the shake table head) on the outside of the carbon dioxide container 1 inch from the bottom of this container. The accelerometer output was fed through a constant gain amplifier to an X-Y plotter. This data is shown in Figure 24 where the accelerometer output is shown as a function of frequency from 35 cps to 3000 cps. It is clear that over this frequency range no significant resonance points are present.

Section 6.0 Summary, Conclusions, and Recommendations

In Table 3 the anticipated characteristics of the solid cryogen refrigerator unit are compared to the measured characteristics of the present unit. In general, the correlation between the predicted characteristics and the measured characteristics are quite excellent. Although the original design might be characterized as being optimistic, it is obvious that a unit can be constructed that closely approximates the design goal. Further, there is little doubt that on the basis of what has been learned with tests on the present unit that the design goals could be met completely.

In the present study it has been conclusively demonstrated that a very simple servicing technique can be utilized for the production of maximum density argon and carbon dioxide in a refrigerator system. This technique involves

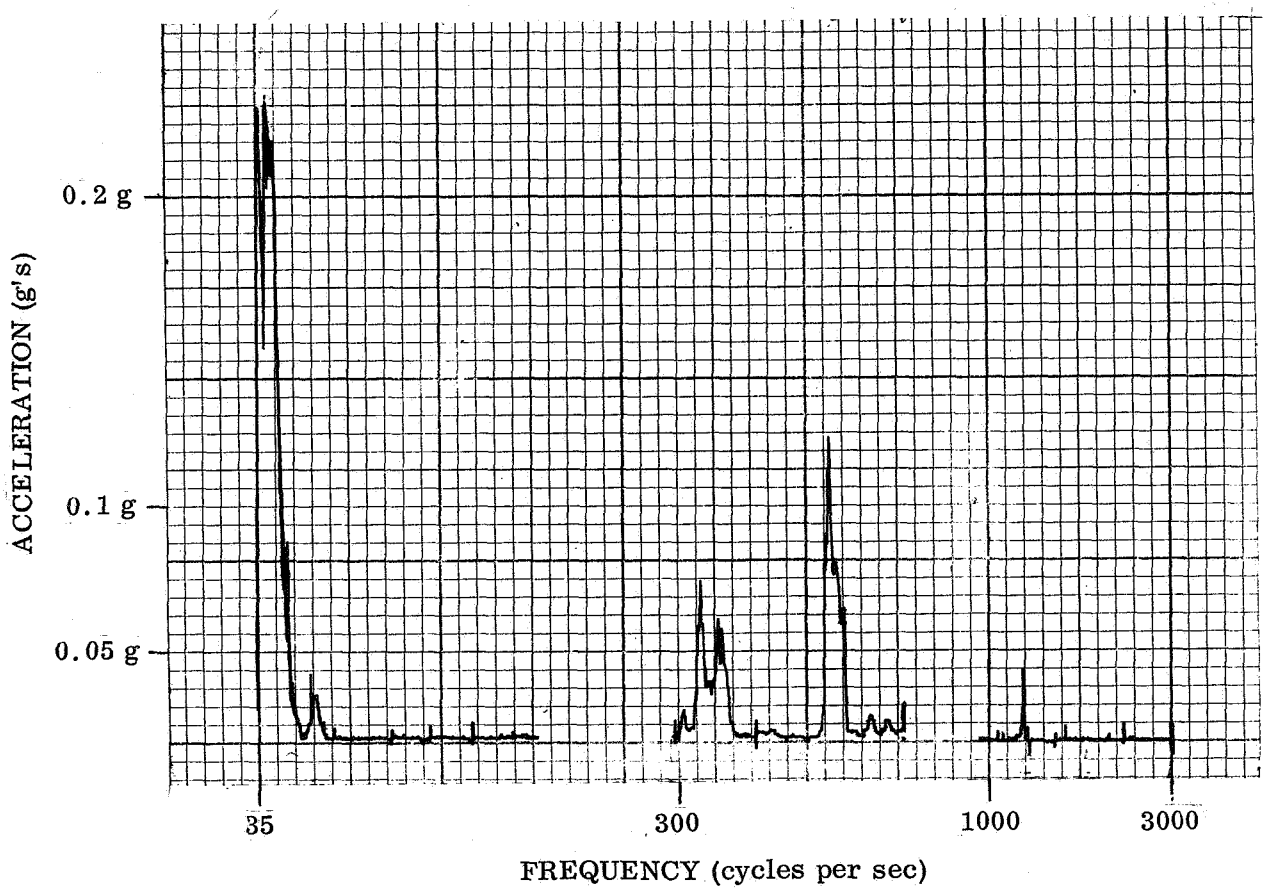

Figure 24. Transverse Acceleration vs. Frequency of Solid Cryogen Refrigeration for 1 g Input Acceleration

Table 3

Predicted vs. Measured Characteristics of Solid Cryogen Refrigerator

	Predicted Value	Measured Value
Detector Operating Temperature	$50^{o}K$	$52^{o}K$
Argon Lifetime	1 year	1 year
Allowable Detector Heat Load	25 mw	17.6 mw
Carbon Dioxide Temperature	$125^{o}K$	$129^{o}K$
Carbon Dioxide Lifetime	1 year	1 year
Heat Leak to Argon	15 mw	28.6 mw
Heat Leak to Carbon Dioxide	76 mw	74 mw
Refrigerator Weight Including Cryogens	29.9 lbs	34.1 lbs

the introduction of gaseous argon and carbon dioxide in the solid cryogen refrigerator within a specified sub-atmospheric pressure range along with the circulation of liquid nitrogen through heat exchangers within the refrigerator unit. The use of a gaseous argon and carbon dioxide filling technique allows the same tubes to be used both as fill and vent lines. The cryogen fill and solidification operation requires a total of about 8 hours; 4 hours are required to complete the fill operation while approximately 4 additional hours are required to completely solidify the argon and subcool the solid to liquid nitrogen temperature. After the initiation of a pumping operation on the $80^{\circ}K$ solid argon 2 hours are required to cool it to within $2^{\circ}K$ of its final operating temperature of $51.9^{\circ}K$. Altogether a 24 hour pumping operation is required for the argon temperature to reach the equilibrium value of $51.9^{\circ}K$.

The passive detector temperature regulation system used in the present refrigerator results in a detector temperature change of $0.028^{\circ}K$ per milliwatt variation in the detector heat load. As the argon in the refrigerator is exhausted there is a drift in the detector operation temperature, as well as the detector temperature regulation. With approximately 3 per cent of the argon left in the refrigerator the detector operating temperature is $52.6^{\circ}K$ and the detector temperature changes $0.037^{\circ}K$ per milliwatt change in the detector heat load.

The thermal capacity of the total masses of argon and carbon dioxide are rather large in terms of the heat loads on these cryogens. In fact, the carbon dioxide temperature rises approximately $3^{\circ}K$ per day from its initial temperature of $80^{\circ}K$, immediately at the completion of the filling operation, to its final operating temperature of $129^{\circ}K$. A period of approximately 17 days results in which no carbon dioxide venting is required. The argon temperature under a no venting condition would only rise approximately $1^{\circ}K$ per day. Since the triple point of argon is at $83.9^{\circ}K$ for each degree Kelvin of sub-cooling below this point the argon could remain unvented and in a solid state. Thus, the present refrigerator is capable of remaining unvented not only during the spacecraft boost phase, but also, for several days of a spacecraft and ground hold phase. Introduction of gaseous helium into the vacuum space surrounding the refrigerator unit results in complete boiloff of the cryogens in the refrigerator in less than 4 hours time.

The structure of the present refrigerator unit has been designed to withstand spacecraft boost acceleration and vibration. Thus, the thermal performance of this unit should be identical to that of a flight model. This is a very important consideration as the structures required to withstand the stringent spacecraft boost vibration and acceleration environment do not possess good thermal characteristics in terms of thermal isolation requirements. The only weak link in the refrigerator structure was the inability under test of a representative main support column to withstand a load greater than that equivalent to a 15 g load on the refrigerator unit. This column did support the required loads of 30 g's under tension and 10 g's under lateral loads. However, on the basis of the reported properties of the glass filament wound epoxy support structure used this column should support 30 g's in compression with a reasonable safety factor. Poorly manufactured columns with possible structural imperfections were apparently the problem in the present system.

The weight of the present unit could have been reduced without any changes in the materials used in the construction in the following manners. The weight of solder used to join the external liquid nitrogen heat exchangers to the argon and carbon dioxide cans was 1.53 lbs. This weight could be eliminated entirely by placing the heat exchangers inside the containers in mechanical contact with the exterior wall of the container. Additionally, this procedure would result in smooth exterior container walls thereby decreasing the absorbtance of these walls for thermal radiation by eliminating possible interreflection of this radiant energy. The heat exchanger tubes thermselves have a total weight of 1 lb. These tubes are stainless steel having a 10 mil wall. Their wall thickness could easily be reduced to 3 mils, a weight saving of 0.7 lbs. The flanges for the main support column with a present weight of 1.5 lbs could be reduced in weight at least 0.6 lbs without reducing their structural characteristics. These measures would reduce the present system weight approximately 2.8 lbs. These measures would leave the basic refrigerator weight less cryogens at about 10 lbs.

The next possible weight reduction would be fabrication of the cryogen containers and internal foam heat exchangers from aluminum which would reduce the system weight by approximately 3 lbs. A system weighing approximately 29 lbs for the present detector cooling requirements would appear to be

as light as is feasible. It should be indicated that since methane has a latent heat of vaporization almost exactly equal to that of argon, that the present system utilizing methane instead of argon as the primary coolant would have the same detector cooling lifetime as the present unit for identical detector heat loads. On the other hand, methane has a density approximately 1/3 that of argon (See Table 4 for a comparison of the properties of methane and argon).

Table 4

Comparison of Properties of Argon and Methane

Cryogen	Operating Temperature in Present Refrigerator	Latent Heat of Sublimation (Cal/cm^3)	Density (g/cm^3)
Argon	52^oK	82.6	1.711
Methane	65^oK	73.8	0.52

Thus with methane the weight of the present system would be reduced 9.1 lbs. The same amount of detector cooling capacity would be available as with the argon unit but the detector operating temperature would be 65^oK or higher. The servicing techniques for a methane unit would be identical to those used in the present argon refrigerator. Based on the present refrigerator characteristics a methane unit with identical detector cooling capacity, with a total system weight of 20 lbs., appears feasible.

The detector cooling capacity of the present unit could be improved in two ways. First as discussed in Section 5.0 an extraneous heat leak to the argon container of 7.2 mw has been identified as radiation heat transfer between the carbon dioxide temperature shroud and the argon container. Some reduction can be afforded in this heat transfer as has been previously indicated by relocating the liquid nitrogen heat exchanger on the inside of the argon container. However, the greatest reduction of this heat transfer

will undoubtedly come from exercising greater quality control in the gold plating operation on the cryogen container including a procedure for verifying the infrared reflection properties of this surface. Infrared emittance inspection devices* are available for measuring the properties of these surfaces. Also, at present there is a rather large thermal load on the detector thermal link due to its present characteristic dimensions. It would be advisable to reduce the surface area of this element by greatly reducing its diameter. With the rather large thermal conductivity of copper the thermal link need only be about 1/16 inch in diameter to support the required detector heat load with negligible temperature drop down its length. On the other hand, some finite area is required for mounting the detector and its matched load resistor. The best system for the detector mount would appear to be a taunt wire suspension. The detector then would be mounted on a small copper plate supported concentrically from a surrounding metal ring by wires under tension. The use of 2 mil. diameter titanium alloy wires would allow firm support and yet a total heat load on the detector support of 1 mw for an 8 wire support system with each supporting wire being 1/2 inch long. The titanium wires in this case are assumed to suspend the nominally $50^{\circ}K$ detector support plate from a metal ring at approximately $300^{\circ}K$. The cooling for the detector mounting plate would be supplied through a short fine flexible copper wire running from the 1/16 inch diameter copper link to the detector mounting plate. This system would maintain the detector at the focus of an optical system even as the refrigerator and detector are cooled from room temperature to $50^{\circ}K$.

*An Optical Surface Comparitor, for example, manufactured by the Lion Research Corporation allows rapid emittance measurements to be made on complex structures such as the present cryogen containers.

7.0 References

Cited References

1. J. M. Toth, Jr. and J. R. Barber, "Structural Properties of Glass-fiber Filament Wound Cryogenic Pressure Vessels," Adv. in Cryogenic Eng. Vol. 10, Plenum Press, 1964, pp 134-143.
2. Thermophysical Properties of Plastic Materials and Composites to Liquid Hydrogen Temperature, AF ML-TDR-64-33, June 1964.
3. "Determination of the Performance of Plastic Laminates under Cryogenic Temperatures," AST TDR 62-794.
4. "Thermophysical Properties of Insulating Materials," ML TDR 64-5.
5. Caren, R.P., "Low Temperature Emittance Determinations,in Thermophysical and Temperature Control of Spacecraft," Progress in Astronautics and Aeronautics, Vol. 18, Academic Press 1966.
6. W. T. Ziegler, J. C. Mullins, and B. S. Kirk, Calculation of the Vapor Pressure and Heats of Vaporization and Sublimation of Liquids and Solids Especially Below One Atmosphere, II. Argon, Engineering Experiment Station, Georgia Institute of Technology, 1962.
7. W. T. Ziegler, J. C. Mullins, and B. S. Kirk, Calculation of the Vapor Pressure and Heats of Vaporization and Sublimation of Liquids and Solids Especially Below One Atmosphere, V. Carbon Monoxide and Carbon Dioxide, Engineering Experiment Station, Georgia Institute of Technology, 1963.

General References

G. K. White, Experimental Techniques in Low Temperature Physics, Oxford Univwity Press, 1962.

R. B. Scott, Cryogenic Engineering, D. Van Nostrand & Co., 1959.

Wright Air Development Division, A Compendium of the Properties of Materials at Low temperature, Phase I Parts 1 and 2, Phase II, WADD TR 60-56, 1960.

A. H. Shapiro, The Dynamics and Thermodynamics of Compressible Fluid Flow, Ronald Press Company, Vol. 1, 1953, p. 228.

R. H. Kropschot, Cryogenic Insulation, (Paper presented at the Cryogenic Conference of the ASHRAE Annual Meeting, Lake Placid, N.Y., June 1959)

Linde Company, Linde Company Superinsulation Applied to Space Vehicles

A. G. Emslie, The Problems of Seams and Penetrations in Panels of Multilayer Foil Insulation, NASA Contract NAS 5-664, ADL No. 63270-04-04.

A. D. Little, Inc., Third and Fourth Progress Reports - Liquid Propellant Losses During Space Flight, NASA Contract NAS 5-664, ADL No. 63270-00-03

National Advisory Committee for Aeronautics, A Simplified Method of Elastic-Stability Analysis for Thin Cylindrical Shells, by S. B. Batdorf, NACA Rept. 874, Washington, D.C. 1947.

J. L. Christian, Physical and Mechanical Properties of Pressure Vessel Materials for Application in a Cryogenic Environment, Aeronautical Systems Division ASD-TDR-62-258, Wright-Patterson Air Force Base, Ohio, Mar. 1962.

R. F. Crawford and A. B. Burns, "Minimum Weight Potentials and Design Information for Stiffened Plates and Shells," American Rocket Society paper ARC-2424-62, Phoenix, Ariz., Apr. 1962.

Lockheed Missiles & Space Company, Structural Shell Optimization Studies, Vol. II, Optimization of Stiffened Cylindrical Shells Subjected to Uniform External Hydrostatic Pressure, by E. H. Nickell and R. F. Crawford, 3-42-61-2, Sunnyvale, Calif., 30 Jun 1961

Holter, et al, Fundamentals of Infrared Technology, MacMillan Co., 1962

H. W. Thompson, Advances in Spectroscopy, Interscience Publishers, Inc., 1959.

NASA-Langley, 1967 —— 23 CR-988